Taylor & Francis
Taylor & Francis Group

Spectroscopy Letters

An International Journal for Rapid Communication

ISSN: (Print) (Online) Journal homepage: https://www.tandfonline.com/loi/lstl20

Synthesis and photoluminescence analysis of europium(III) complexes with pyrazole acid and nitrogen containing auxiliary ligands

Jyoti Khanagwal , S. P. Khatkar , Priyanka Dhankhar , Manju Bala , Rajesh Kumar , Priti Boora & V. B. Taxak

To cite this article: Jyoti Khanagwal , S. P. Khatkar , Priyanka Dhankhar , Manju Bala , Rajesh Kumar , Priti Boora & V. B. Taxak (2020): Synthesis and photoluminescence analysis of europium(III) complexes with pyrazole acid and nitrogen containing auxiliary ligands, Spectroscopy Letters, DOI: 10.1080/00387010.2020.1817093

To link to this article: https://doi.org/10.1080/00387010.2020.1817093

Published online: 18 Sep 2020.

SPECTROSCOPY LETTERS
https://doi.org/10.1080/00387010.2020.1817093

Taylor & Francis
Taylor & Francis Group

Synthesis and photoluminescence analysis of europium(III) complexes with pyrazole acid and nitrogen containing auxiliary ligands

Jyoti Khanagwal[a], S. P. Khatkar[a], Priyanka Dhankhar[a], Manju Bala[a], Rajesh Kumar[b], Priti Boora[a] and V. B. Taxak[a]

[a]Department of Chemistry, Maharshi Dayanand University, Rohtak, India; [b]University Institute of Engineering and Technology (UIET), Maharshi Dayanand University, Rohtak, India

ABSTRACT

Four red photoluminescent europium(III) complexes have been synthesized by using fluorinated carboxylate ligand, 1-(4-methoxyphenyl)-5-(trifluoromethyl)-1*H*-pyrazole-4-carboxylic acid as main ligand and bathophenanthroline, 1,10-phenanthroline and 2,2-bipyridyl as auxiliary ligands, through solution precipitation approach. The complexes possess an optimum thermal stability, which is sufficient for organic light emitting diodes fabrication. Under ultraviolet excitation, the complexes display an intense emission peak of europium ion, which makes them a promising red color emitter in display devices. Internal quantum efficiency, color coordinates, Judd–Ofelt parameters, and energy transfer mechanism have been explored. The investigated antimicrobial and antioxidant activity suggest that the synthesized complexes are potent antimicrobial and antioxidant agents.

RESEARCH HIGHLIGHTS

- A new ligand L has been synthesized by an ecofriendly method.
- Four Eu(III) complexes have been synthesized through a facile solution precipitation method by using ligand L and auxiliary ligands.
- CHN, EDAX, IR, NMR, TG-DTG, DR, UV–vis, and PL spectroscopic techniques and antioxidant analysis are employed.
- Potential candidate for display devices, laser devices, and antimicrobial agents.

ARTICLE HISTORY
Received 21 August 2020
Accepted 22 August 2020

KEYWORDS
Antioxidant; luminescence; Judd–Ofelt parameters; optical; spectroscopic

Introduction

Up to now, a surge of investigations by material scientists is accelerating on lanthanide luminescent materials day by day owing to their interesting optoelectronic properties such as high luminescence efficiency, static luminescent location, long luminescence decay time, and good color purity,[1] which endorsed their potential applications in display systems, solid state lighting systems[2] mainly white organic light emitting diodes (W-OLEDs),[3] security inks and tags,[4] biomedical sensors, optical cell imaging,[5] and biological systems.[6] Therefore, the synthesis and the development of lanthanide chelates with high luminescence efficiency have become a hot research topic at present time. The luminescence of lanthanide ion is associated with 4f–4f electronic transitions in ultra-visible and near-infrared region. As a consequence of parity rule, 4f–4f electronic transitions are laporte forbidden transitions, which are responsible for low molar absorptivity and less possibility of direct excitation of lanthanide ion. This inconvenience can be controlled by coordinating the central lanthanide ion to the light harvesting organic chromophores, which sensitize the lanthanide ion by antenna effect. On the other hand, the luminescence efficiency is also determined by the energy transfer process from the excited triplet energy levels of organic ligand to the emissive level of lanthanide ion and better compatibility between both energy levels directly improves the luminescence efficiency of lanthanide ion.[7] Currently, among different types of organic ligands, one of the most promising light harvesting chromophores, fluorinated aromatic carboxylic acid

CONTACT V. B. Taxak v_taxak@yahoo.com Department of Chemistry, Maharshi Dayanand University, Rohtak, India.

ligand containing extended π-conjugation, more binding modes, high thermal, and light stability, attracts much attention for complexation with lanthanide ion.[1,8] The organic ligands possessing C–F oscillators diminish the energy loss in non-radiative decay process and facilitate the energy transfer mechanism.[9] It can be acknowledged that the high-energy O–H, N–H, and C–H oscillators of solvent and binding ligands in coordination sphere quench the metal excited states through non-radiative decay process leading to shorter lifetime of excited states resulting into lower photoluminescence efficiency of lanthanide complexes.[10] But the solvent molecules get easily substituted by highly conjugated N-containing auxiliary ligands, which control non-radiative decay process via synergistic effect.[11] Also, auxiliary ligands provide high rigidity, chemical stability, and satisfy the coordination environment around lanthanide ion.[12] Among lanthanide ions, the europium(III) ion gains burgeoning attention due to environment independent line like emission at 615 nm and long luminescent decay time.

Keeping the above facts in mind, the main fluorinated aromatic carboxylic acid, 1-(4-methoxyphenyl)-5-(trifluoromethyl)-1*H*-pyrazole-4-carboxylic acid (L) and its corresponding europium(III) complexes, $Eu(L)_3.2H_2O$ (C1), $Eu(L)_3$.batho (C2), $Eu(L)_3$.phen (C3), and $Eu(L)_3$.bipy (C4) have been synthesized by using bathophenanthroline (batho), 1,10-phenanthroline (phen), and 2,2-bipyridyl (bipy) as auxiliary ligands, through solution precipitation approach. The synthesized ligand (L) and europium(III) complexes are characterized by various techniques, energy dispersive X-ray analysis (EDAX), elemental analysis, proton nuclear magnetic resonance (^{1}H-NMR), carbon nuclear magnetic resonance (^{13}C-NMR), Fourier transform infrared (FT-IR), ultraviolet–visible absorption (UV–vis), thermogravimetric (TG) and differential thermogravimetric (DTG) analyses, diffuse reflectance (DR), scanning electron microscopy (SEM), and photoluminescence spectroscopy (PL). The luminescence parameters such as radiative lifetime (τ), non-radiative rate (A_{nrad}), radiative rate (A_{rad}), Judd–Ofelt parameters (Ω_λ), and internal quantum efficiency (η) are explained in detail. The energy transfer mechanism explicates the luminescence efficiency of the complexes and biological investigations suggest that the synthesized complexes are potent antimicrobial and antioxidant agents. The synthesized europium(III) complexes are considered as potential candidates in laser and solar technology, advanced luminescent devices, new electronic technology, and fabrication of tricolor based white light emitting diodes. The pyrazole-based complexes play a great role for inhibition of growth of microbes, therefore, the complexes exhibit promising applications in the biological and pharmacological fields.

Experimental

Materials and methods

A series of luminescent europium(III) complexes were synthesized through a facile solution precipitation method by utilizing highly pure (99.9%) europium(III) nitrate pentahydrate, 2,2-bipyridyl, bathophenanthroline, and 1,10-phenanthroline. The chemicals and solvents used in the synthesis of complexes and ligand were of high purity and analytical reagent grade. The chemicals were purchased from easily available commercial source, Merck (Mumbai, India) and used as such without further purification. 2,2-Diphenyl-1-picrylhydrazyl hydrate (DPPH) and ascorbic acid consumed in the estimation of antioxidant property of complexes were purchased from Central drug house (CDH), New Delhi, India. The double-distilled water was used for the synthesis of complexes.

Carbon, hydrogen and nitrogen (CHN) analysis were performed on Perkin Elmer 2400 CHN elemental analyzer (PerkinElmer, Waltham, MA) and EDAX analysis was done on Ametek EDAX. The complexometric titration with ethylenediaminetetraacetic acid (EDTA) was used to detect the europium(III) ion content in the complexes. The FT-IR spectra of europium(III) complexes and ligand (L) were recorded with the help of Perkin Elmer Spectrum 400 spectrometer (PerkinElmer, Waltham, MA) in wavenumber range of 4000–400 cm^{-1}, by dispersing the solid sample on dry KBr disks. ^{1}H-NMR and ^{13}C-NMR of

complexes were recorded on Bruker Avance II 400 NMR spectrometer (Bruker, Fremont, CA) in deutrated dimethylsulfoxide (d^6-DMSO) solvent with respect to reference tetramethylsilane (TMS) while ^{13}C-NMR of ligand (L) was recorded in $CDCl_3$ (deuterated chloroform). UV–vis absorption and solid diffuse reflectance spectral analysis of ligand (L) and complexes were performed on Shimadzu UV-3600 plus UV–visible spectrophotometer (Shimadzu, Kyoto, Japan) in wavelength range of 200–800 nm. Thermogravimetric investigation was done on SDT Q600 thermal analyzer under inert atmosphere of N_2 gas with the heating rate of 20 °C/min. The morphological features were assessed by using Jeol JSM-6510 SEM (JEOL Ltd., Tokyo, Japan). Furthermore, the phosphorescence and luminescence spectral data was collected on Hitachi F-7000 fluorescence spectrophotometer (Hitachi, Shiga, Japan) employed with xenon lamp, which acted as a source of radiations. The decay curves of europium complexes were determined by using software (FL solution of F-7000) of the spectrophotometer and color coordinates were calculated with the help of MATLAB software. The biological properties such as antimicrobial and antioxidant were investigated through tube dilution and DPPH methods, respectively.

Synthesis of ligand 1-(4-methoxyphenyl)-5-(trifluoromethyl)-1H-pyrazole-4-carboxylic acid (L)

The ligand L was synthesized in three step as shown below (Fig. 1a)-[13]:

Step 1: Synthesis of ethyl 2-((*N*-trifluoromethyl-*N*-methylamino)methylene)-3-oxobutanoate: ethylacetoacetate (0.2 mL) was stirred along with continuous dropwise addition of N-(dimethoxymethyl)-1,1,1-trifluoro-*N*-methylmethanamine (0.3 mL) at room temperature. The reaction mixture was left for about 16 hr with constant stirring at room temperature and then evaporated under reduced pressure. The resulting product was purified by chromatography, which produced the oily substance of ethyl 2-((N-trifluoromethyl-*N*-methylamino)methylene)-3-oxobutanoate.

Step 2: Synthesis of ethyl 1-(4-methoxyphenyl)-5-(trifluoromethyl)-1*H*-pyrazole-4-carboxylate: 4-methoxyphenyl hydrazine (0.15 mL) and ethyl 2-((*N*-trifluoromethyl-*N*-methylamino)methylene)-3-oxobutanoate (0.978 mmol) were dissolved in ethanol (5 mL) and refluxed for about 3 hr, then evaporated under reduced pressure. The obtained residue was dissolved in ethyl acetate, washed three times with saturated aqueous solution of sodium bicarbonate, and subsequently extracted with ethyl acetate. The extracts were dried with the help of anhydrous magnesium sulfate ($MgSO_4$) and then evaporated under reduced pressure. The oily product of ethyl 1-(4-methoxyphenyl)-5-(trifluoromethyl)-1*H*-pyrazole-4-carboxylate is obtained after purification of extracts through chromatography.

Step 3: Synthesis of 1-(4-methoxyphenyl)-5-(trifluoromethyl)-1*H*-pyrazole-4-carboxylic acid (L): Ethanolic (2 mL) solution of potassium hydroxide (4.07 mmol) and ethyl 1-(4-methoxyphenyl)-5-(trifluoromethyl)-1*H*-pyrazole-4-carboxylate (0.604 mmol) was refluxed for about 6 hr. The resulting mixture was allowed to evaporate under reduced pressure. The aqueous solution of hydrochloric acid (6 N) was added to obtained residue to adjust the pH ~1 resulting into white solid was separated which was extracted with ethyl acetate and dried over anhydrous $MgSO_4$. The solid product was purified by chromatography to obtain the pure white solid 1-(4-methoxyphenyl)-5-(trifluoromethyl)-1*H*-pyrazole-4-carboxylic acid (L) and progress of reaction was checked by thin layer chromatography. 78% yield of product (L) was received with 166 °C melting point. IR (KBr): cm^{-1} 3443 (b), 2967 (w), 2850 (w), 2764 (w), 2363 (w), 1709 (s), 1604 (s), 1564 (s), 1462 (s), 1423 (s), 1374 (m), 1305 (s), 1255 (s), 1183 (s), 1144 (s), 1074 (s), 1025 (s), 962 (s), 922 (s), 838 (s), 777 (s), 744 (m), 667 (m), 603 (m), 546 (s), 508 (w) 446 (w); ^{1}H-NMR (DMSO, 400 MHz): δ 3.85 (s, 3H, -OCH_3), 7.09–7.12 (d, 2H, Ar-H), 7.45–7.47 (d, 2H, Ar-H), 8.21 (s, 1H, pyrazole−C−H), 13.31 (s, 1H, −COOH) ppm; ^{13}C-NMR (100 MHz, $CDCl_3$): δ 55.6 (O−CH_3), 114.3 (Ar−C−C = O), 127.1 (Ar−CH), 132.1 (Ar−CN), 143.03 (pyrazole−CH), 160.6 (−COOH) ppm. Anal. Cal.

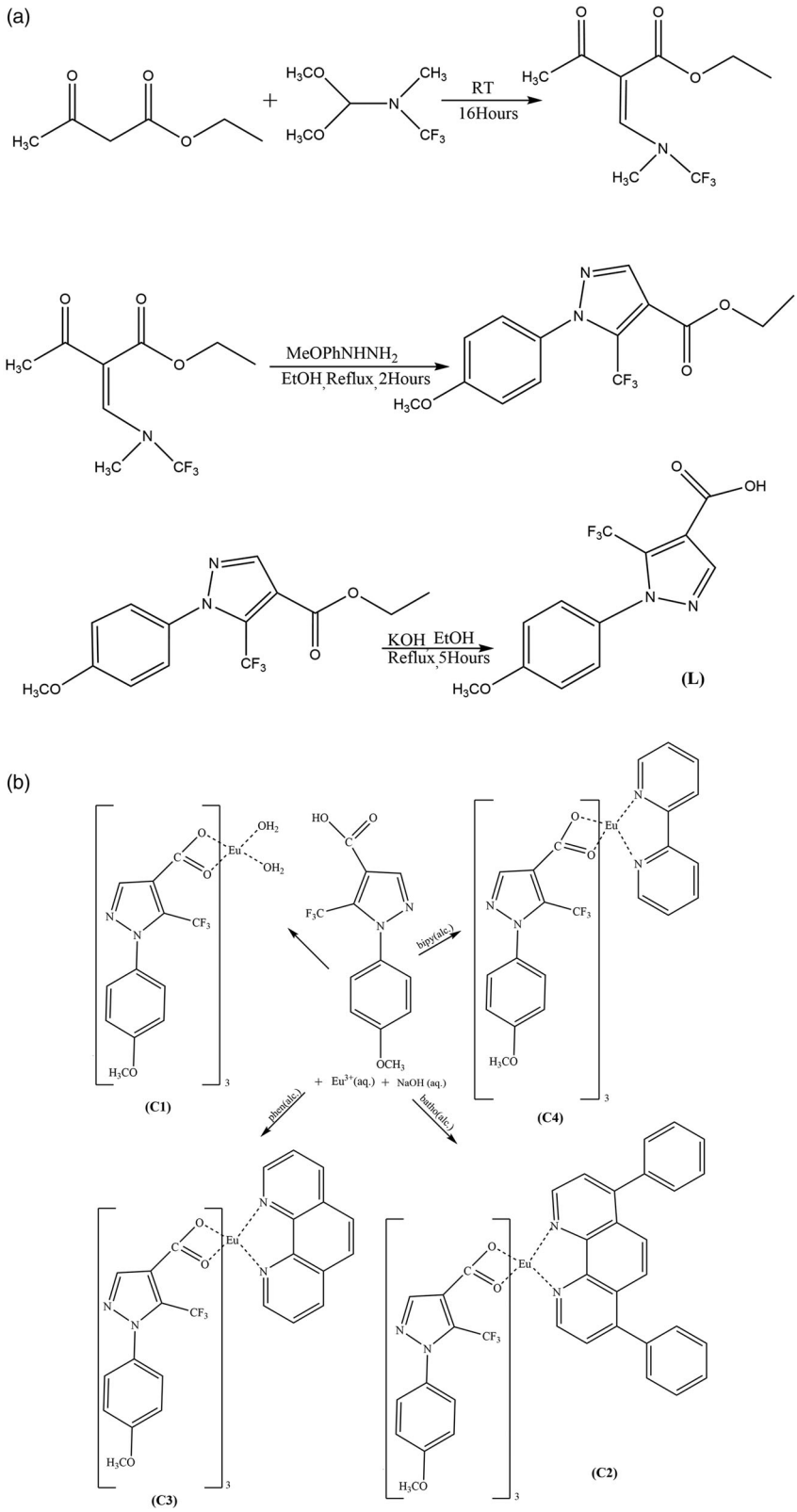

Figure 1. Synthetic methods and chemical structures of [13] ligand 1-(4-methoxyphenyl)-5-(trifluoromethyl)-1*H*-pyrazole-4-carboxylic acid (a) and europium(III) complexes C_1–C_5 (b). The ligand gets deprotonated on addition of alkali solution and deprotonated ligand is coordinated to europium(III) ion at ~7 pH value.

for $C_{12}H_9N_2O_3F_3$: C, 50.36; H, 3.17; N, 9.79; found: C, 50.32; H, 3.14; N, 9.78.

Synthesis of europium(III) complexes

Ethanolic solution of ligand (3 mmol) was added to aqueous solution of europium nitrate (1 mmol) with constant stirring on magnetic stirrer at room temperature. The pH of resulting solution was adjusted in the range of 6–7 with the addition of dilute NaOH solution (0.05 M) dropwise. Furthermore, the reaction mixture was stirred for about 4 hr on the magnetic stirrer. The obtained white crude product was filtered on suction pump and subsequently washed with water, then with ethanol three times to remove unreacted ligand from the reaction mixture. The filtered precipitates were dried in oven and finally in vacuum desiccator to obtain the white powder of C1 complex (Fig. 1b).

$Eu(L)_3.(H_2O)_2$ (C1): White solid, yield 70%; IR (KBr): cm^{-1} 3409 (b), 3005 (w), 2936 (w), 2838 (w), 2359 (w), 2341 (w), 1640 (w), 1582 (m), 1564 (s), 1519 (s), 1463 (w), 1432 (s), 1404 (w), 1327 (s), 1301 (w), 1292 (m), 1257 (s), 1228 (w), 1180 (s), 1137 (s) , 1080 (m), 1040 (s), 971 (s), 836 (s), 799 (s), 749 (w), 683 (w), 630 (w), 604 (w), 546 (m), 507 (w), 478 (w), 464 (w); ^{1}H-NMR (400 MHz, DMSO): δ 3.78 (s, 9H, $-OCH_3$), 6.99 (s, 3H, pyrazole –C−H), 7.13–7.14 (d, 12H, Ar-H) ppm; ^{13}C-NMR (100 MHz, DMSO): δ 55.6 (O-CH_3), 114.7 (>C = O), 124.7 (CF_3), 131.8 (Ar -CN), 138.8 (pyrazole−CH) ppm. Anal. Cal. for EuC_{36} $H_{28}N_6O_{11}F_9$: C, 41.43; H, 2.70; N, 8.05; Eu, 14.56; found: C, 41.41; H, 2.67; N, 8.08; Eu, 14.58.

The similar approach was adopted for the synthesis of C2–C4 complexes along with the addition of ethanolic solution of auxiliary ligands, bathophenanthroline (1 mmol), 1,10-phenanthroline (1 mmol) and 2,2-bipyridyl (1 mmol), respectively, in the resulting solution of aqueous europium nitrate (1 mmol) and ethanolic solution of ligand (3 mmol). To illustrate the triplet energy level of ligand, the gadolinium complex of ligand L [$Gd(L)_3.2H_2O$] (G_1) was also synthesized by adopting similar strategy as used for C1 complex.

$Eu(L)_3$.batho (C2): White powder, yield 78%; IR (KBr): cm^{-1} 3008 (w), 2942 (w), 2839 (w), 2362 (w), 2338 (w), 1640 (m), 1614 (s), 1581 (m), 1567 (s), 1552 (m), 1518 (s), 1492 (w), 1461 (m), 1439 (s), 1402 (s), 1326 (s), 1292 (s), 1255 (s), 1228 (m), 1182 (s), 1140 (s), 1078 (m), 1039 (s), 970 (s), 834 (s), 800 (s), 764 (m), 748 (w), 701 (w), 644 (w), 628 (w), 604 (m), 572 (w), 545 (m), 505 (w), 478 (w), 464 (w); ^{1}H-NMR (DMSO, 400 MHz): δ 3.76 (s, 9H, -OCH_3), 6.94–7.07 (d, 6H, Ar-H), 7.75 (s, 14H, Ar-H), 8.04 (s, 3H, pyrazole−C−H), 8.32–8.54 (d, 6H, Ar-H), 9.02–9.09 (s, 2H, Ar-H) ppm; ^{13}C-NMR (100 MHz, DMSO): δ 55.4 (O−CH_3), 113.9 (Ar−C−C = O), 124.2 (−CF_3), 127.1 (Ar−CH), 131.7 (Ar−CN), 137.6 (pyrazole−CH), 147.2–156.4 (Ar−C=C−), ppm. Anal. Cal. for $EuC_{60}H_{40}N_8O_9F_9$: C, 53.78; H, 3.01; N, 8.36; Eu, 11.34; found: C, 53.76; H, 3.02; N, 8.34; Eu, 11.32.

$Eu(L)_3$.phen (C3): White solid, yield 75%; IR (KBr): cm^{-1} 3005 (w), 2961 (w), 2936 (w), 2839 (w), 2360 (w), 2340 (w), 1639 (m), 1620 (s), 1590 (s), 1565 (s), 1553 (m), 1519 (s), 1462 (m), 1430 (s), 1401 (w), 1324 (s), 1313 (s), 1293 (s), 1254 (s), 1230 (m), 1179 (s), 1134 (s), 1080 (m), 1038 (s), 971 (s), 863 (w), 841 (s), 800 (s), 768 (w), 749 (w), 701 (w), 668 (w), 630 (w), 603 (w), 572 (w), 547 (m), 507 (w), 477 (w), 465 (w); ^{1}H-NMR (DMSO, 400 MHz): δ 3.77 (s, 9H, $-OCH_3$), 6.96–7.11 (d, 6H, Ar-H), 7.47 (s, 8H, Ar-H), 7.96 (s, 3H, pyrazole−C−H), 8.40–8.41(d, 4H, Ar-H), 8.70 (s, 2H, Ar-H) ppm; ^{13}C-NMR (100 MHz, DMSO): δ 55.4 (O−CH_3), 113.9 (Ar−C−C = O), 124.2 (−CF_3), 127.1–127.6 (Ar−CH), 131.7 (Ar−CN), 137.3 (pyrazole−CH), 142.1–159.6 (Ar−C=C−) ppm. Anal. Cal. for $EuC_{48}H_{32}N_8O_9F_9$: C, 48.54; H, 2.72; N, 9.43; Eu, 12.79; found: C, 48.55; H, 2.71; N, 9.41; Eu, 12.79.

$Eu(L)_3$.bipy (C4): White solid, yield 76%; IR (KBr): cm^{-1} 3004 (w), 2959 (w), 2936 (w), 2837 (w), 2360 (w), 2341 (w), 1640 (w), 1619 (s), 1563 (s), 1518 (s), 1494 (w), 1461 (m), 1431 (s), 1401 (w), 1323 (s), 1292 (m), 1252 (s), 1231 (m), 1175 (s), 1137 (s), 1079 (s), 1040 (s), 970 (s), 833 (s), 800 (s), 766 (s), 741 (s), 703 (s), 664 (w), 628 (m), 603 (w), 574 (w), 546 (m), 505 (w), 478 (w), 464 (w); ^{1}H-NMR (400 MHz, DMSO): δ 3.76 (s, 9H, $-OCH_3$), 6.95–7.07 (d, 6H, Ar-H), 7.76 (s, 10H, Ar-H), 8.03 (s, 3H, pyrazole−C−H),

8.32–8.54 (d, 4H, Ar-H) ppm; ^{13}C-NMR (100 MHz, DMSO): δ 55.4 (O−CH_3), 113.5 (Ar−C−C = O), 124.3 (−CF_3), 127.3–127.7 (Ar−CH), 131.5 (Ar−CN), 137.6 (pyrazole−CH), 141.4–152.3 (Ar−C=C−) ppm. Anal. Cal. for $EuC_{46}H_{32}N_8O_9F_9$: C, 47.48; H, 2.77; N, 9.63; Eu, 13.06; found: C, 47.50; H, 2.76; N, 9.62; Eu, 13.05.

$Gd(L)_3.(H_2O)_2$ (G1): White solid, yield 60%; IR (KBr): cm^{-1} 3412 (b), 3009 (w), 2936 (w), 2838 (w), 2359 (w), 2343 (w), 1642 (w), 1582 (m), 1564 (s), 1552 (m), 1520 (s), 1463 (w), 1431 (s), 1404 (w), 1327 (s), 1302 (w), 1292 (m), 1257 (s), 1228 (w), 1182 (s), 1137 (s) , 1080 (m), 1040 (s), 971 (s), 836 (s), 799 (s), 749 (w), 683 (w), 630 (w), 604 (w), 546 (m), 507 (w), 478 (w), 464 (w). Anal. Cal. for GdC_{36} $H_{28}N_6O_{11}F_9$: C, 41.22; H, 2.69; N, 8.01; Gd, 14.99; found: C, 41.19; H, 2.66; N, 7.99; Gd, 15.01.

Biological properties

In vitro *antimicrobial properties*

The antibacterial activity of the complexes and ligand (L) was assessed against Gram-positive and Gram-negative bacterial pathogens named as *Staphylococcus aureus* (*S. aureus*), *Escherichia coli* (*E. coli*), and *Pseudomonas aeruginosa* (*P. aeruginosa*), respectively, whereas the antifungal activity was evaluated against fungal pathogens such as *Aspergillus niger* (*A. niger*) and *Candida albicans* (*C. albicans*). The ciprofloxacin and fluconazole were used as the standard drugs for estimation of antibacterial and antifungal activity, respectively. The dilutions of standard drugs, ligand and complexes were done by dissolving in ethanol to prepare 100 µg/mL concentration of solutions and resulting solutions were left for incubation The incubation periods for different pathogens were 24 hr at 37 °C (bacteria), 7 days at 25 °C, and 48 hr at 37 °C for *A. niger* and *C. albicans*, respectively. The mediums such as double strength nutrient broth I.P. (Indian Pharmacopoeia) for antibacterial and Sabouraud dextrose I.P. for antifungal activity were employed for in vitro investigations. The antimicrobial activity was determined in terms of minimum inhibitory concentration (MIC) of samples, which clearly pointed out that the minimum quantity of complexes was sufficient to prevent the growth of bacteria and fungi, thereby, can be employed as commercial bactericidal and fungicides.[14] The complexes can be used as excellent bactericidal and fungicides.

In vitro *antioxidant activity*

2,2-Diphenyl-1-picrylhydrazyl hydrate (DPPH) nitrogen centered stable free radical method was employed to investigate the antioxidant activity of ligand and its corresponding europium complexes. The antioxidant activity of complexes was studied by reaction of DPPH with antioxidant samples in which the purple color of DPPH solution convert to yellow color, which produced a significant absorbance at 517 nm with the help of UV–vis spectrophotometer. The stock solutions of tested samples and standard sample (ascorbic acid) were prepared with different concentrations such as 25 µg/mL, 50 µg/mL, 75 µg/mL, and 100 µg/mL in ethanol. Then, 1 mL solution of each concentration of different samples and standard sample was mixed with 1 mL DPPH solution (3 µg/mL) in their respective flasks and DPPH solution was considered as control. After that, the mixtures were thoroughly stirred and kept for incubation in dark for 30 min. After the completion of incubation period, the absorbance of different mixtures was recorded at 517 nm against blank then it converted into percentage scavenging activity by using Eq. (1). These investigations were carried out in triplicate containing 99 blocks. IC_{50} (concentration implementing 50% inhibition) values of samples were obtained from the curve, which is plotted between percentage scavenging activity (% SCA) and various concentrations of tested samples.

The scavenging activity of DPPH was estimated by given equation[15]:

$$\begin{aligned} &Scavenging\ activity\ (\%) \\ &= [(Abs_{control} - Abs_{sample})/Abs_{control}] \times 100 \end{aligned} \quad (1)$$

where $Abs_{control}$ signifies the absorbance of DPPH + ethanol and Abs_{sample} represents the absorbance of DPPH + sample or standard.

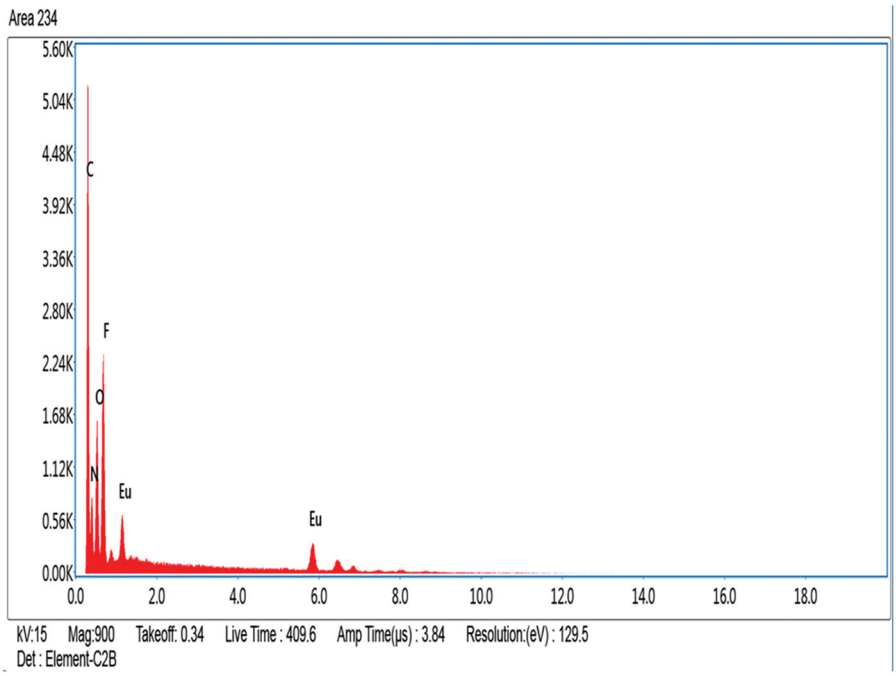

Figure 2. Energy dispersive X-ray spectrum of C_4 complex of europium(III) ion with main ligand 1-(4-methoxyphenyl)-5-(trifluoromethyl)-1*H*-pyrazole-4-carboxylic acid and auxiliary ligand 2,2-bipyridyl. The spectrum confirms the presence of carbon, nitrogen, oxygen, fluorine and europium elements in C_4 complex.

Table 1. Percentage analytical data (weight %) of free ligand 1-(4-methoxyphenyl)-5-(trifluoromethyl)-1*H*-pyrazole-4-carboxylic acid (main ligand), C1 complex of europium(III) ion with main ligand and complexes C2–C4 with main ligand and auxiliary ligands bathophenanthroline, 1,10-phenanthroline and 2,2-bipyridyl, respectively.

Complexes	C (%) found (Cal.)	H (%) found (Cal.)	N (%) found (Cal.)	Eu (%) found (Cal.)
L	50.32 (50.36)	3.14 (3.17)	9.78 (9.79)	–
C1 $[Eu(L)_3.2H_2O]$	41.41 (41.43)	2.67 (2.70)	8.08 (8.05)	14.58 (14.56)
C2 $[Eu(L)_3.batho]$	53.76 (53.78)	3.02 (3.01)	8.34 (8.36)	11.32 (11.34)
C3 $[Eu(L)_3.phen]$	48.55 (48.54)	2.71 (2.72)	9.41 (9.43)	12.79 (12.79)
C4 $[Eu(L)_3.bipy]$	47.50 (47.48)	2.76 (2.77)	9.62 (9.63)	13.05 (13.06)

L: 1-(4-methoxyphenyl)-5-(trifluoromethyl)-1*H*-pyrazole-4-carboxylic acid; batho: bathophenanthroline; phen: 1,10-phenanthroline; bipy: 2,2-bipyridyl; C: carbon; H: hydrogen; N: nitrogen; Eu: europium; Cal: calculated. The calculated data are closed to the experimentally recorded (found) data.

Results and discussion

Compositions and properties of complexes

The EDAX analysis authenticates the elemental compositions (carbon, nitrogen, oxygen, fluorine, and europium) possessed by the complexes, which is illustrated by EDAX spectrum of C4 complex (Fig. 2). The CHN and complexometric titration results (Table 1) are in good consonance with each other, which clearly justify that the molecular compositions of complexes are in accordance with proposed formulae of the synthesized complexes as given in Scheme 2. All the europium complexes are soluble in DMSO, partially soluble in chloroform, acetonitrile, and ethanol while insoluble in diethyl ether.

Spectral analysis

The FT-IR spectra of ligand (L) (Fig. 3a) and europium(III) complexes show a remarkable differences. The spectra of all complexes C1–C4 resemble to each other indicating that the similar mode of coordination in complexes, therefore, IR spectrum of complex C4 is depicted in Fig. 3b as representative of all complexes. The characteristic absorption frequencies of ligand (L) and complexes are displayed in Table 2. The absorption bands of uncoordinated ligand (L) are situated at 1709, 1564, and 1183 cm^{-1} corresponding to stretching vibrations of >C=O, >C=N, and C–F groups, respectively. The IR spectrum of ligand (L) displays the absorption bands at 1305 and 1144 cm^{-1}, which are related to stretching

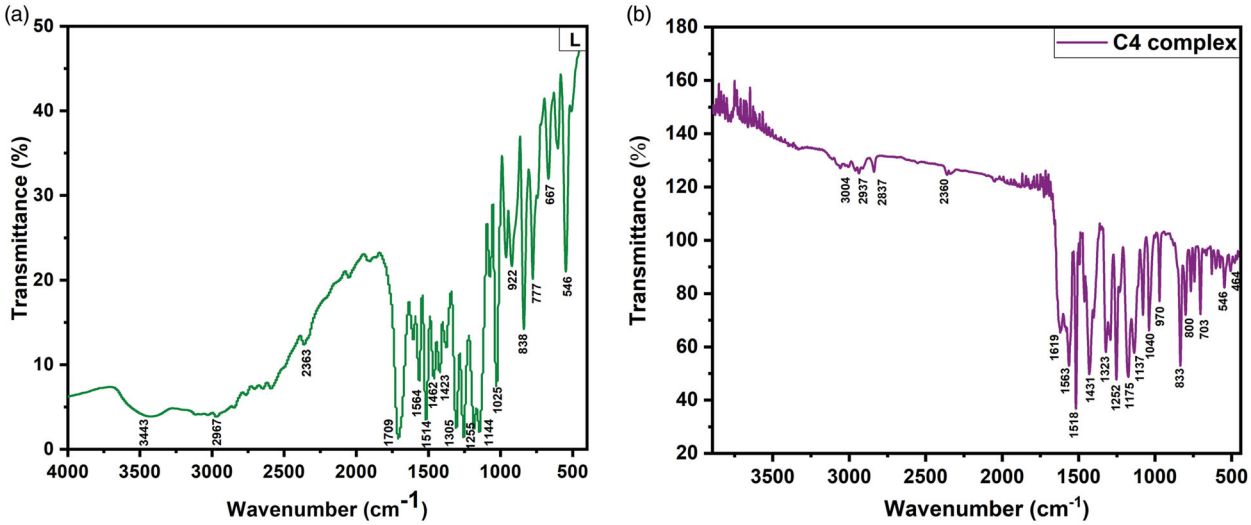

Figure 3. Infrared spectra of free ligand 1-(4-methoxyphenyl)-5-(trifluoromethyl)-1*H*-pyrazole-4-carboxylic acid (a) and europium(III) complex C4 (b) with main ligand 1-(4-methoxyphenyl)-5-(trifluoromethyl)-1*H*-pyrazole-4-carboxylic acid and auxiliary ligand 2,2-bipyridyl. The coordination of auxiliary ligand 2,2-bipyridyl and main ligand to europium(III) ion is confirmed by the spectral peaks in C_4 complex.

Table 2. The characteristics infrared spectral frequencies (cm^{-1}) of uncoordinated ligand 1-(4-methoxyphenyl)-5-(trifluoromethyl)-1*H*-pyrazole-4-carboxylic acid (main ligand) and its corresponding complexes, C1 complex of europium(III) ion with main ligand and C2–C4 complexes with main ligand and auxiliary ligands bathophenanthroline, 1,10-phenanthroline and 2,2-bipyridyl, respectively.

Complexes	ν (O–H)	ν (C=O)	ν_{asym} (OCO)	ν_{sym} (OCO)	ν (C=N)	ν (C–F)	ν (Eu–N)	ν (Eu–O)
L	3443 (b)	1709 (s)	–	–	1564 (s)	1183(s)	–	–
C1 [Eu(L)$_3$.2H$_2$O]	3409 (b)	–	1582 (m)	1432 (s)	1564 (s)	1180 (s)	–	464 (w)
C2 [Eu(L)$_3$.batho]	–	–	1614 (s)	1439 (s)	1567 (s)	1182 (s)	572 (w)	464 (w)
C3 [Eu(L)$_3$.phen]	–	–	1620 (s)	1430 (s)	1565 (s)	1179 (s)	572 (w)	465 (w)
C4 [Eu(L)$_3$.bipy]	–	–	1619 (s)	1431 (s)	1563 (s)	1175 (s)	574 (w)	464 (w)

L: 1-(4-methoxyphenyl)-5-(trifluoromethyl)-1H-pyrazole-4-carboxylic acid; batho-bathophenanthroline, phen-1,10-phenanthroline; bipy: 2,2-bipyridyl; ν: frequency of bands; b: broad; s: strong; m: medium; w: weak; sym: symmetric stretching; asym: asymmetric stretching. The changes in stretching frequencies affirm that the auxiliary ligands and deprotonated ligand are coordinated to europium(III) ion.

vibrations of C–N and N–N bonds, respectively. The broad band at 3443 cm^{-1} corresponding to stretching vibrations of –OH of carboxylic acid group (–COOH) in IR spectrum of free ligand (L) while the broad band at 3409 cm^{-1} in the spectrum of C1 complex is ascertained to –OH groups of coordinated water molecules in C1 complex. This broad band vanishes in C2–C4 complexes, showing successfully substitution of water molecules by auxiliary ligands. The characteristic absorption band of >C=O group in complexes is also disappeared while two extra asymmetric ($\nu_{asym,}$ COO^-) and symmetric ($\nu_{sym,}$ COO^-) absorption bands of carboxylate group occur in the range of 1582–1614 and 1430–1439 cm^{-1}, suggesting the coordination of carboxylate group in bidentate manner with the central Eu^{3+} ion as the difference of ($\nu_{asym,}$ COO^-) and ($\nu_{sym,}$ COO^-) is found in the range of 150–190 cm^{-1} (<225 cm^{-1}).[16] In IR spectra of free ligand (L) and C1 complex, the band (1564 cm^{-1}) corresponding to >C=N group of pyrazole ring is slightly shifted by 1–3 cm^{-1} in IR spectra of C2–C4 complexes (1563–1567 cm^{-1}), which may be due to overlapped bands of >C=N group of pyrazole ring and auxiliary ligands. This overlapped band confirms the coordination of auxiliary ligands to trivalent europium ion (Eu^{3+}) in C2–C4 complexes. Furthermore, the absorption bands present in the range of 572–574 cm^{-1} and 464–465 cm^{-1} in complexes can be accredited to Eu-N and Eu-O, respectively, pointing out that Eu^{3+} ion is coordinated through carboxylate group of main ligand (L) and nitrogen atoms of auxiliary ligands.[17,18]

The ^{1}H and ^{13}C-NMR spectra of ligand and europium(III) complexes are recorded in deutrated dimethyl sulfoxide (d^6-DMSO) solvent at

room temperature. The ^{1}H-NMR spectra of Eu(III) complexes in comparison of spectra of free ligand (L) show remarkable changes. The characteristic absorption peaks of ligand at δ 13.31, 8.21, 7.45–7.47, and 3.85 ppm are accredited to –OH of carboxylic acid group, pyrazole ring proton, aromatic protons and methoxy ($-OCH_3$) group, respectively Fig. 4a. The absorption peaks at δ 8.21 and 3.85 ppm are shifted to upfield in the range of δ 6.99–8.04 and 3.76–3.78 ppm, respectively, and most of peaks are broadened upon coordination in the complexes suggesting the paramagnetic character of Eu^{3+} ion. The absorption peak at δ 13.31 ppm of ligand disappears in complexes clearly reveal that Eu^{3+} ion coordinates with ligand (L) through carboxylate group. The appearance of extra aromatic peaks ranging from δ 7.75–9.09 ppm in ^{1}H-NMR spectra of C2–C4 complexes substantiates the coordination of auxiliary ligands to europium(III) ion in C2–C4 complexes. The complex C3 acts as depictive of all the complexes because the spectral profiles of all the complexes are alike, hence, ^{1}H-NMR spectrum of C3 complex is manifested in Fig. 4b. ^{13}C-NMR peaks of ligand (L) are positioned at δ 143.0, 132.1, 127.1, and 55.6 ppm corresponding to pyrazole –CH, Ar–CN, Ar–CH, and $-OCH_3$ groups, respectively, which are shifted to higher field on complexation as compared to free ligand (L) pointing out the paramagnetic chemical environment around Eu^{3+} ion. The peak at δ 160.6 ppm due to –COOH group in ^{13}C-NMR spectrum of ligand (L) is not visible in the complexes, which indicates that the ligand L is coordinated to Eu^{3+} ion through carboxylate group. Hence, the above analyses of IR, ^{1}H-NMR, and ^{13}C-NMR spectroscopy are in agreement with each other.

UV–visible absorption spectroscopy

The UV–vis absorption spectra of ligand (L) and Eu(III) complexes (C1–C4) are manifested in Fig. 5. The absorption maxima of ligand (L) is obtained at 259 nm corresponding to $\pi \rightarrow \pi^*$ electronic transitions of ligand whereas the absorption maxima of complexes are located at 265 nm (C1), 273 nm (C2–C3), and 282 nm (C4). This shift in absorption maxima (6–23 nm) of complexes C1–C4 toward higher wavelength region suggests the energy gap between HOMO (highest occupied molecular orbital) and LUMO (lowest unoccupied molecular orbital) decreases upon coordination, which results into more effective energy transfer from ligand to Eu^{3+} ion.[19]

Band-gap analysis

The plot of absorption coefficient with photon energy is obtained from the diffused reflectance (DR) data by special calculation. The spectral profile of europium(III) complexes (C1–C4) are identical, hence, C4 complex acts as depictive of all complexes C1–C4. The plots of absorption coefficient against photon energy for ligand (L) and its respective europium(III) complexes are demonstrated in Fig. 6a, b, respectively, while their respective diffuse reflectance spectra are displayed in insets of these figures. The optical energy band-gap (E_g) values of complexes are determined by transformation of diffused reflectance spectra as shown by Kubelka and Munk and it is narrated by employing the general equation as given below[20]:

$$[F(R_\infty)h\nu]^n = C(h\nu - E_g) \tag{2}$$

In the above equation, E_g denotes the energy of band-gap, C represents the constant of proportionality, h denotes Planck' constant and ν designates the frequency of incident radiation. The values of exponent n for indirect allowed transition, direct allowed, indirect forbidden and direct forbidden transition are 0.5, 2, 3, and 1.5, respectively. The symbol $F(R_\infty)$ signifies the Kubelka–Munk function whose value is demarcated as[20]:

$$F(R_\infty) = \frac{(1-R_\infty)^2}{2R_\infty} = \frac{K}{S} \tag{3}$$

where R_∞ symbolizes the ratio of $R_{normal}/R_{standard}$ while K and S presents the absorption and scattering coefficient, respectively. The optical energy band-gap (E_g) of ligand and complexes are calculated by extrapolating a tangent against photon energy (hυ) with $[F(R_\infty)h\nu]^2 = 0$ in Tauc plots. The optical band-gap energy of C1–C4 complexes (3.98–3.37 eV) are found to be less than that of

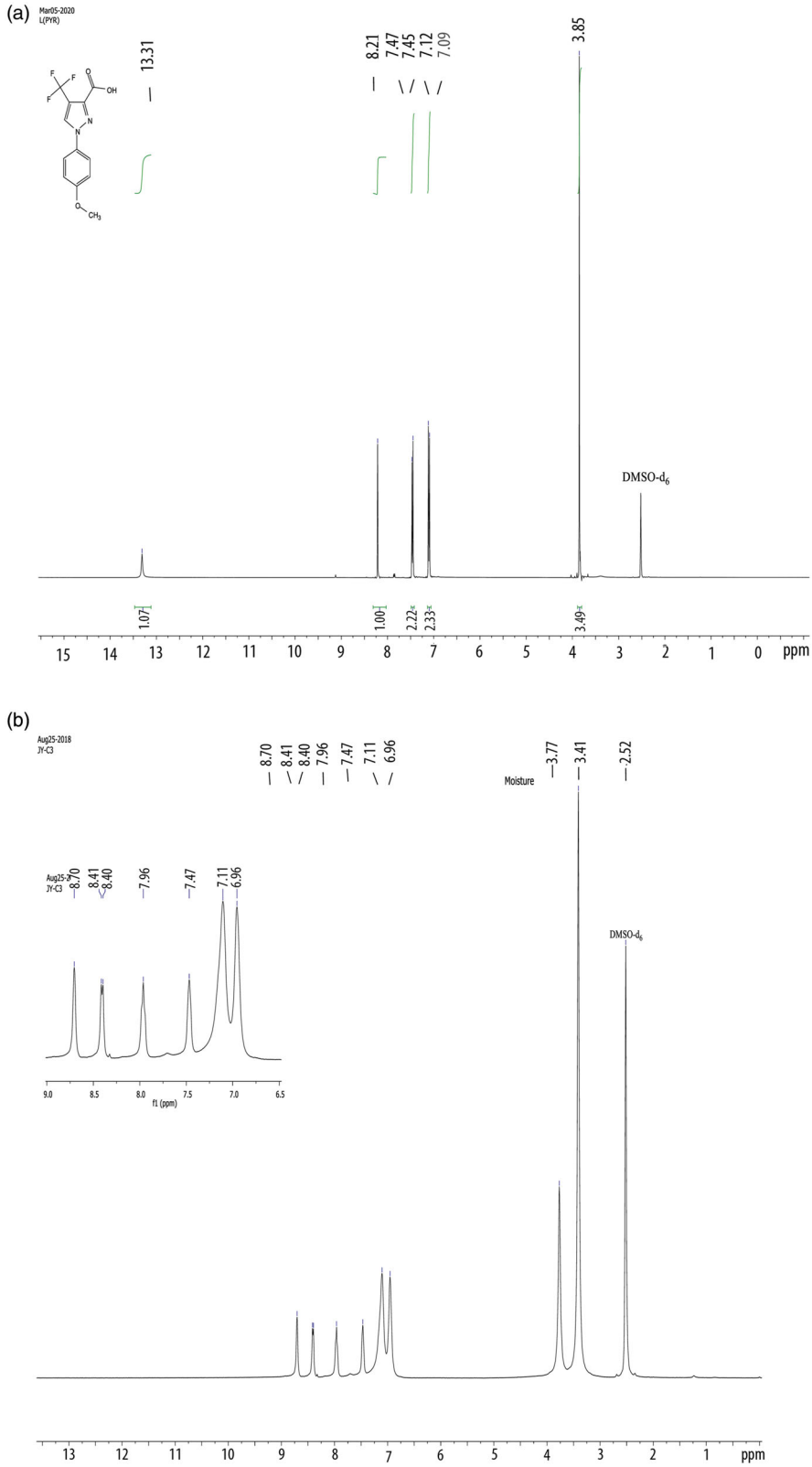

Figure 4. Proton nuclear magnetic resonance spectra of free ligand 1-(4-methoxyphenyl)-5-(trifluoromethyl)-1*H*-pyrazole-4-carboxylic acid (a) and C_3 complex of europium(III) ion (b) with main ligand 1-(4-methoxyphenyl)-5-(trifluoromethyl)-1*H*-pyrazole-4-carboxylic acid and auxiliary ligand 1,10-phenanthroline recorded in deuterated dimethyl sulfoxide solvent. The spectral profile of C_3 complex suggest that the main ligand is coordinated to europium(III) ion after removal of proton.

ligand (5.63 eV), which confirms the decrease of energy difference between HOMO and LUMO. This decrease results into more effective energy transfer from ligand to excited levels of Eu(III) ion. Further, the band-gap energy range (3.98–3.37 eV) of complexes (C1–C4) is in accordance with the energy gap (2–4 eV) of wide band-gap semiconductors (WBGs). Therefore, the complexes are considered as worthy contender in lasers, military radars and energy converting systems. Nowadays, according to the energy department of US (United State), these europium(III) complexes can be employed as efficient semiconductors for developing the new electrical technologies and alternate energy devices.[21]

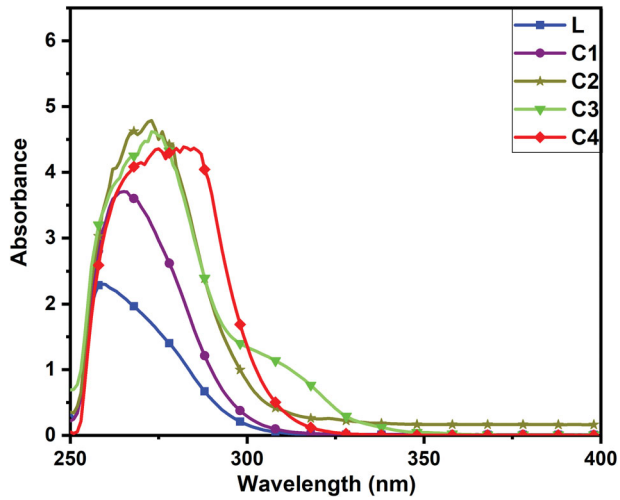

Figure 5. Absorption spectra of ligand 1-(4-methoxyphenyl)-5-(trifluoromethyl)-1*H*-pyrazole-4-carboxylic acid (main ligand), C_1 complex of eupoium(III) ion with main ligand and C_2–C_4 complexes with main ligand and auxiliary ligands bathophenanthroline, 1,10-phenanthroline and 2,2-bipyridyl, respectively, recorded in dimethyl sulfoxide solvent. The absorption spectra of complexes display the red shift as compared to ligand.

Thermal analysis

The thermal stability of europium(III) complexes (C1–C4) has been investigated by thermogravimetric (TG) and differential thermogravimetric (DTG) analyses from ambient temperature to 800 °C in the presence of nitrogen gas flow. All europium(III) complexes exhibit the similar order of thermal decomposition, hence, the decomposition pattern of C4 complex is considered as representative of all complexes as shown in Fig. 7. The TG curve of complex represents the loss of moisture (3.47%) in first step. The complex starts to decompose at 152 °C and ends up to 572 °C, which leads to removal of one auxiliary ligand bipy and three main organic ligands (L) with weight loss of 86.98%. The theoretical and calculated values are found to be close to the total mass loss of complex. At last, europium oxide is leftover as final residue. The above fact suggests that these luminescent complexes have optimum thermal stability up to 152 °C, hence, the complexes can be acted as emitting materials in OLEDs fabrication.[10]

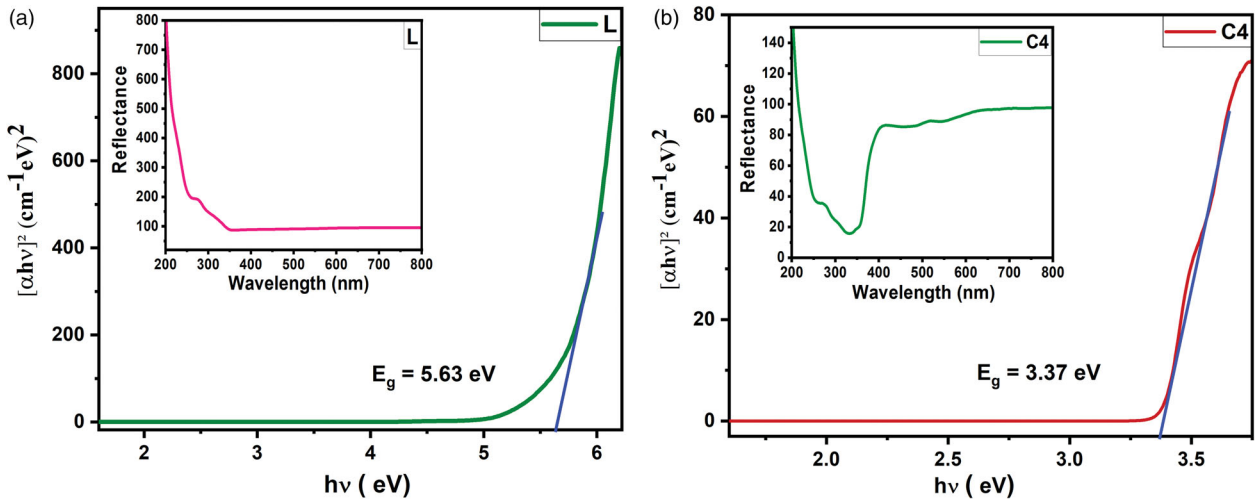

Figure 6. Tauc plots of main ligand 1-(4-methoxyphenyl)-5-(trifluoromethyl)-1*H*-pyrazole-4-carboxylic acid (a) and C_4 complex of europium(III) ion with main ligand and auxiliary ligand 2,2-bipyridyl (b) while their insets display the corresponding diffuse reflectance spectra. The plots illustrate the decreasing of energy difference between highest occupied molecular orbital and lowest unoccupied molecular orbital in C_4 complex on the basis of band-gap energy.

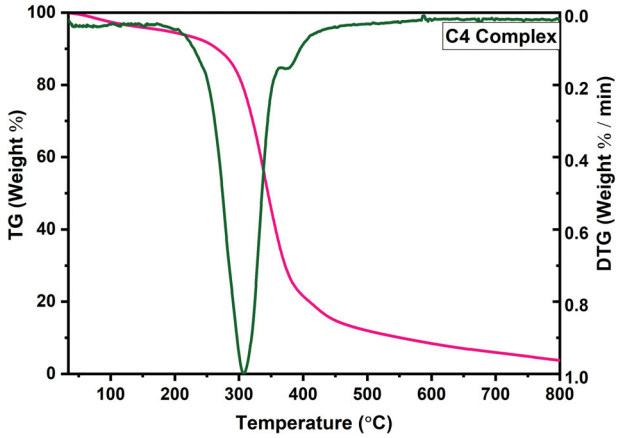

Figure 7. Thermogravimetric and differential thermogravimetric curves of complex C_4 of europium(III) ion with main ligand 1-(4-methoxyphenyl)-5-(trifluoromethyl)-1*H*-pyrazole-4-carboxylic acid and auxiliary ligand 2,2-bipyridyl documented under inert atmosphere of dinitrogen gas. The curves indicate that the complex C_4 possess an optimum thermal stability (152 °C).

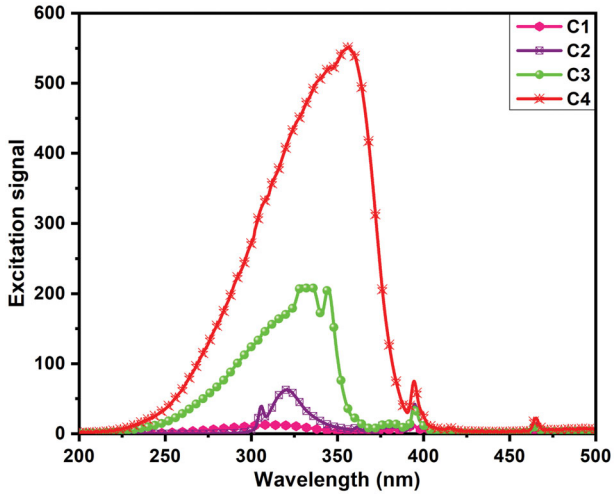

Figure 8. Solid state excitation spectra of C_1 complex of europium(III) ion with main ligand 1-(4-methoxyphenyl)-5-(trifluoromethyl)-1*H*-pyrazole-4-carboxylic acid and C_2–C_4 complexes with main ligand and auxiliary ligands such as bathophenanthroline, 1,10-phenanthroline and 2,2-bipyridyl, respectively, recorded by fixing the wavelength of intense emission peak. The wavelengths of excitation maxima are scrutinized as 320 nm (C_1), 321 nm (C_2), 344 nm (C_3), and 356 nm (C_4).

Photoluminescence characterization

To analyze the photoluminescence properties of luminescent Eu(III) complexes, the excitation spectra of complexes are recorded by fixing $^5D_0 \rightarrow {}^7F_2$ prominent emission transition of Eu^{3+} ion, in 200–500 nm range with 400 PMT voltage as displayed in Fig. 8. One can find that the excitation spectra of the complexes consist of bands in two regions, a remarkable broad band in higher energy region (200–370 nm) with maxima at different wavelengths for the corresponding complexes such as 320 nm (C1), 321 nm (C2), 344 nm (C3), and 356 nm (C4), which can successfully be accredited to $\pi \rightarrow \pi^*$ ligand centered transition. The lower energy region (358–470 nm) of excitation spectra of complexes contains the less intense peaks at 361, 375, 382, 395, and 465 nm, which are allocated to $^7F_0 \rightarrow {}^5D_4$, $^7F_0 \rightarrow {}^5G_2$, $^7F_0 \rightarrow {}^5G_3$, $^7F_0 \rightarrow {}^5L_6$, and $^7F_0 \rightarrow {}^5D_2$ characteristics transitions of Eu^{3+} ion.[22,23]

Further, the emission spectra of europium(III) complexes are scanned at room temperature within the range of 400–700 nm on applying the maximal excitation wavelength of corresponding complexes C1–C4. The emission spectra of Eu(III) complexes (Fig. 9) are composed of emission peaks at 580, 592, 614 (C1) and 615 (C2–C4), 657 (C1–C2, C4), 661 (C3) and 698 (C1–C3), 699 nm (C4), which are ascribed to $^5D_0 \rightarrow {}^7F_0$, $^5D_0 \rightarrow {}^7F_1$, $^5D_0 \rightarrow {}^7F_2$, $^5D_0 \rightarrow {}^7F_3$, and $^5D_0 \rightarrow {}^7F_4$ transitions, respectively.[24] The weak emission peaks corresponding to $^5D_1 \rightarrow {}^7F_0$, $^5D_1 \rightarrow {}^7F_1$, $^5D_1 \rightarrow {}^7F_2$ transitions centered at 526, 536 and 554 (C1–C2, C4), 555 nm (C3) are observed in the spectra of C1–C4 complexes, which are presented in inset of Fig. 9 (C3–C4 complexes) for clear inspection of transitions. In addition, a diminished peak at 468 nm assigned to $^5D_2 \rightarrow {}^7F_0$ transition is also discernible in emission spectra of complexes. Among these emission peaks, the most prominent peak located at 615 nm (C2–C4) and 614 nm (C1) emanates from induced electric dipole allowed transition $^5D_0 \rightarrow {}^7F_2$, which corresponds to bright red emission of Eu^{3+} ion. The magnetically allowed dipole transition ($^5D_0 \rightarrow {}^7F_1$) is insensitive to site symmetry whereas the emission signal corresponding to electric dipole transition ($^5D_0 \rightarrow {}^7F_2$) is extremely sensitive to local symmetry around Eu^{3+} ion in the coordination sphere. The transitions $^5D_0 \rightarrow {}^7F_0$ and $^5D_0 \rightarrow {}^7F_3$ are parity forbidden transitions according to selection rule while $^5D_0 \rightarrow {}^7F_4$ transition is electronically allowed transition and the peak corresponding to this transition shows stark splitting, which supports the asymmetric environment around Eu^{3+} ion. Of

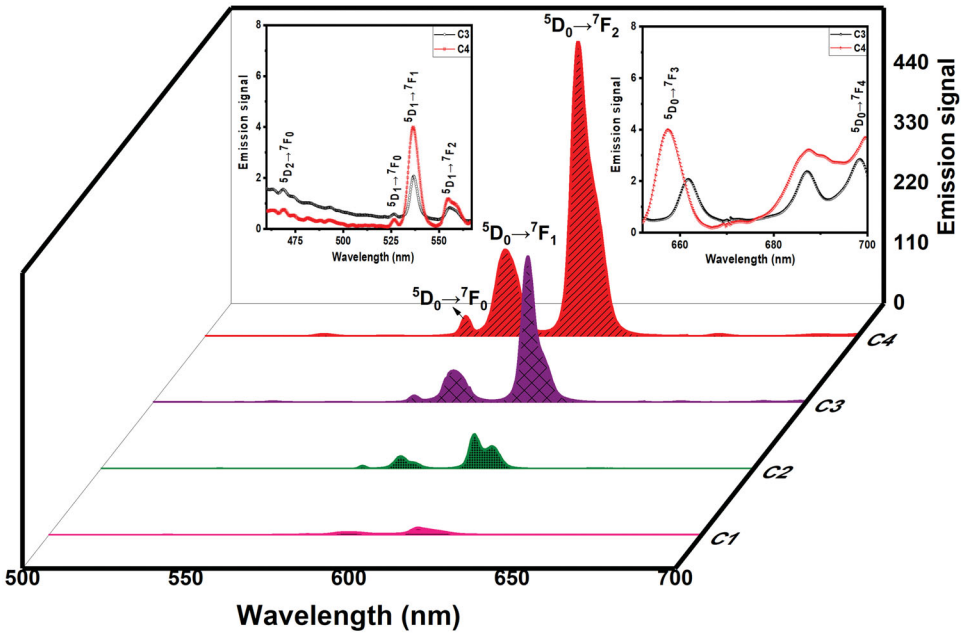

Figure 9. Room temperature emission spectra of C_1 complex of europium(III) ion with main ligand 1-(4-methoxyphenyl)-5-(trifluoromethyl)-1*H*-pyrazole-4-carboxylic acid and C_2–C_4 complexes with main ligand and auxiliary ligands such as bathophenanthroline, 1,10-phenanthroline and 2,2-bipyridyl, respectively. The graph demonstrate the different transitions emanating from lower energy excited level of europium(III) ion while insets display the less intense peaks corresponding to different transitions which are originated from lower energy and higher energy excited levels of europium(III) ion in C_3 and C_4 complexes.

note, the emission signal with respect to electric dipole ($^5D_0\rightarrow^7F_2$) transition is about three fold stronger than the signal of magnetic dipole transition, which recommends that Eu^{3+} ion is devoid of an inversion center.[25] The C–F oscillators in main ligand (L) reduce energy loss non-radiatively during vibration of organic ligand, which improves the luminescence efficiency of the complexes. It is worthy noted that the photoluminescence emission signal of europium(III) complexes (C2–C4) can be further improved by removing the vibronic quenching produced by high energy O–H oscillators of water molecules present in coordination sphere of C1 complex. This can be removed by incorporation of rigid and highly conjugated auxiliary ligands in coordination sphere in place of water molecules, which can be enhanced the emission signal strength of C2–C4 complexes up to a great extent via synergistic effect.

The percentage branching ratios of luminescent europium(III) complexes are found to be almost greater than 60% with respect to electric dipole transition $^5D_0\rightarrow^7F_2$ as listed in Table 3. The branching ratios are obtained on dividing the integrated area of peak corresponding to $^5D_0\rightarrow^7F_2$ transition by total integrated area of all emission peaks. The branching ratios of the complexes C1–C4 for electric dipole transition ($^5D_0\rightarrow^7F_2$) are laid in the range of 64.41–74.43%, hence, the complexes act as promising candidates in the laser diodes.[26]

The CIE (Commission Internationale de I'Eclairage) color coordinates (x and y) of europium(III) complexes are determined with the help of emission spectral data by using MATLAB software. The chromaticity coordinates of complexes 0.4696, 0.2486 (C1), 0.5691, 0.2956 (C2), 0.6093, 0.3381 (C3), and 0.6403, 0.3462 (C4), respectively, are tabularized in Table 3, which are presented in the x–y plane. The chromaticity coordinates of complexes C1–C4 are well located in red region of chromaticity diagram as demonstrated in Fig. 10. The CIE values of C4 complex are well comparable to SMPTE (Society of Motion Picture and Television, $x = 0.63$, $y = 0.34$) and EBU (European Broadcasting Union, $x = 0.64$, $y = 0.33$) due to high intense red color of this complex, thus, proving to be an excellent red component in OLEDs.[27]

Table 3. Color coordinates, branching ratios with respect to $^5D_0 \rightarrow {}^7F_2$ transition of europium(III) ion and color purity of complex C_1 of europium(III) ion with 1-(4-methoxyphenyl)-5-(trifluoromethyl)-1*H*-pyrazole-4-carboxylic acid as main ligand and complexes C_2–C_4 with main ligand and auxiliary ligands bathophenanthroline, 1,10-phenanthroline and 2,2-bipyridyl, respectively.

Complexes	Color coordinates (*x*, *y*)	$^5D_0 \rightarrow {}^7F_0$	$^5D_0 \rightarrow {}^7F_1$	$^5D_0 \rightarrow {}^7F_2$	$^5D_0 \rightarrow {}^7F_3$	$^5D_0 \rightarrow {}^7F_4$	I_{615}/ I_{592}	CP (%)
C1 [Eu(L)$_3$.2H$_2$O]	(0.4696, .2486)	2.84	25.66	64.41	3.25	3.84	2.51	56.40
C2 [Eu(L)$_3$.batho]	(0.5691, .2956)	2.28	22.89	73.72	0.92	0.19	3.22	61.44
C3 [Eu(L)$_3$.phen]	(0.6093, .3381)	2.21	22.15	73.58	0.56	1.49	3.32	84.64
C4 [Eu(L)$_3$.bipy]	(0.6403, .3462)	2.15	22.06	74.43	0.45	0.91	3.37	93.83

L: 1-(4-methoxyphenyl)-5-(trifluoromethyl)-1*H*-pyrazole-4-carboxylic acid; batho: bathophenanthroline; phen: 1,10-phenanthroline; bipy: 2,2-bipyridy; *x*, *y*: coordinates along *x* and *y*-axis; $^5D_0 \rightarrow {}^7F_0$, $^5D_0 \rightarrow {}^7F_1$, $^5D_0 \rightarrow {}^7F_2$, $^5D_0 \rightarrow {}^7F_3$ and $^5D_0 \rightarrow {}^7F_4$: transitions from lowest excited level ($^5D_0$) to ground levels ($^7F_{J\,=\,0,\,1,\,2,\,3,\,4}$) of europium(III) ion, respectively; CP(%): percentage color purity; I_{615} and I_{592}: integrated areas of emission peaks at wavelengths of 615 nm and 592 nm. The color purity and color coordinates confirm the light emitted by europium complexes.

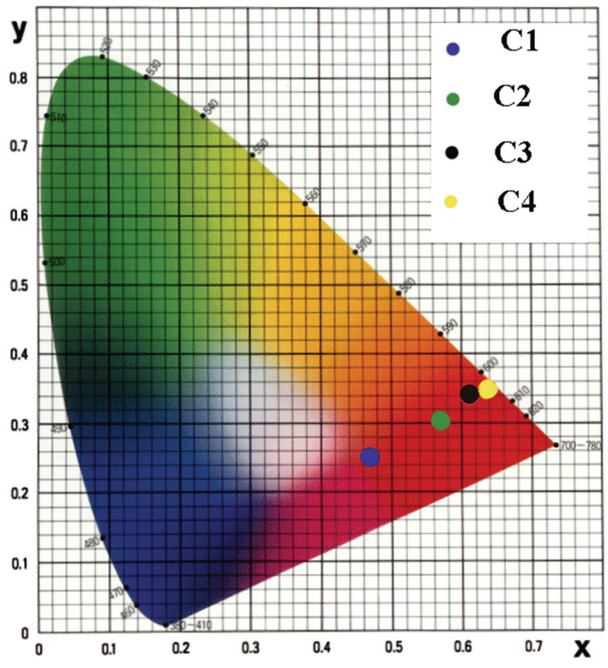

Figure 10. Color coordinates of complex C_1 of europium(III) ion with main ligand 1-(4-methoxyphenyl)-5-(trifluoromethyl)-1*H*-pyrazole-4-carboxylic acid and C_2–C_4 complexes with main ligand and auxiliary ligands bathophenanthroline, 1,10-phenanthroline and 2,2-bipyridyl, respectively, in chromaticity diagram. The chromaticity diagram reveals that the color coordinates of complexes (C1: x = 0.4696, y = 0.2486, C2: x = 0.5691, y = 0.2956, C3: x = 0.6093, y = 0.3381, C4: x = 0.6403, y = 0.3462) lie in red region of chromaticity diagram, which confirm the emitted color of complexes (color figure online).

The color purity (CP) of the complexes is determined with respect to illuminated coordinates (x_i = 0.33, y_i = 0.33) in CIE color gamut space, indicates that how strongly a particular complex may be acted as red color emitter. The color purity is weighted average of dominant emission color coordinates of that sample (x_s, y_s) and dominant wavelength coordinates (x_d, y_d) with respect to standard CIE 1931 illuminated coordinates (x_i, y_i) as shown by the following equation[28]:

$$CP = \sqrt{\frac{(x_s - x_i)^2 + (y_s - y_i)^2}{(x_d - x_i)^2 + (y_d - y_i)^2}} \times 100\% \qquad (4)$$

The color purity (CP) of complexes (C1–C4) is found in the range of 56.40–93.83%, which is enlisted in Table 3. The dominant color purity of C2–C4 complexes is due to presence of auxiliary ligands which intensify the luminescence of these complexes. Hence, the complexes can be considered as red light emitting component in fabrication of tricolor RGB (red, green, and blue) based white organic light emitting diodes (WOLEDs).[29]

To investigate the homogeneous environment around the Eu^{3+} ion, the photoluminescence decay curves of Eu(III) complexes are recorded for $^5D_0 \rightarrow {}^7F_2$ transition and pulsed excitation of corresponding complexes. The photoluminescence decay curves are satisfactory fitted into the first order exponential equation as given below[30]:

$$I = I_\circ \ \exp(-t/\tau) \qquad (5)$$

where exp represents the exponential function, τ symbolizes the lifetime for radiative emission, while I and I_0 are the integrated areas of photoemission peak corresponding to $^5D_0 \rightarrow {}^7F_2$ transition at time t and 0, respectively. The decay curves are well fitted into first-order exponential function, which prove the possibility of homogenous chemical environment around the emitting Eu^{3+} ion[7] as demonstrated in Fig. 11. The decay time values of europium complexes (C1–C4) are found in the range of 0.3893–1.5706 ms as reported in Table 4. The shorter decay time of C1 complex is associated with dominant non-radiative decay channels induced by vibronic coupling of O–H oscillators

of water molecules present in coordination sphere of C1 complex. It is noteworthy pointing that the presence of auxiliary ligands in place of water molecules in C2–C4 complexes is diminished the non-radiative decay channels. This also improves the lifetime (τ) of excited states through radiative decay pathway resulting into an efficient energy transfer from ligands to Eu^{3+} ion.[31]

The luminescent properties of Eu(III) complexes are further assessed by evaluating the internal quantum efficiency (η) of the complexes. The internal quantum efficiency (η) of $^5D_0$ excited level of Eu^{3+} ion is calculated by employing the photoluminescence lifetime (τ) and emission spectral data, which is demarcated by the following equation[32]:

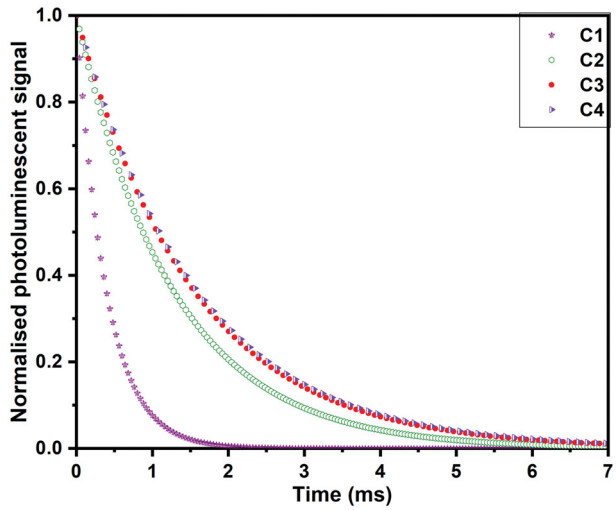

Figure 11. The photoluminescent decay curves of complex C_1 of europium(III) ion with main ligand 1-(4-methoxyphenyl)-5-(trifluoromethyl)-1*H*-pyrazole-4-carboxylic acid and complexes C_2–C_4 with main ligand and auxiliary ligands such as bathophenanthroline, 1,10-phenanthroline and 2,2-bipyridyl, respectively, recorded with respect to wavelength of intense emission peak.

$$\eta = \frac{A_{rad}}{A_{rad} + A_{nrad}} \tag{6}$$

In aforementioned equation, A_{nrad} and A_{rad} represent the non-radiative and radiative decay rate constants, respectively. The internal quantum efficiency (η) helps to investigate the interaction between the radiative and non-radiative decay processes and lies in the range of 7.84–36.69% for C1–C4 complexes (Table 4). It can be noticed that the internal quantum efficiency (η) of C2–C4 complexes is comparatively higher than C1 complex due to the presence of auxiliary ligands which populate the higher excited levels of Eu^{3+} ion by synergistic effect, thus, the complexes support the advanced display devices fabrication.

Further, the radiative and non-radiative decay processes are related to radiative lifetime (τ) according to given equation as expressed below[33]:

$$A_{total} = \frac{1}{\tau} = A_{rad} + A_{nrad} \tag{7}$$

The certain photoluminescence parameters (A_{total}, A_{nrad}, A_{rad}, and η) are tabulated in Table 4. The radiative decay rate (A_{rad}) is evaluated by addition of radiative decay rates of each distinctive transitions $^5D_0 \rightarrow {}^7F_J$ ($J = 0, 1, 2, 3, 4$) of Eu^{3+} ion. The radiative decay rate, A_{06} is not estimated due to absence of emission peak corresponding to $^5D_0 \rightarrow {}^7F_6$ transition. Hence, this radiative rate does not involve in the depopulation of excited level of Eu^{3+} ion. The radiative decay rate (A_{0J}) of each transition can be calculated by using the following equation[34]:

$$A_{0J} = A_{01} \left(\frac{I_{0J}}{I_{01}}\right) \left(\frac{\nu_{01}}{\nu_{0J}}\right) \tag{8}$$

where I_{0J} and ν_{0J} represent the integrated areas of emission peaks and energy barycenter for corresponding $^5D_0 \rightarrow {}^7F_J$ transitions ($J = 0, 1, 2, 3, 4$),

Table 4. Experimentally calculated photoluminescent data of complex C_1 of europium(III) ion with 1-(4-methoxyphenyl)-5-(trifluoromethyl)-1*H*-pyrazole-4-carboxylic acid as main ligand and C_2–C_4 complexes with main ligand and auxiliary ligands bathophenanthroline, 1,10-phenanthroline and 2,2-bipyridyl, respectively.

Complexes	τ (ms)	A_{total} (s^{-1})	A_{rad} (s^{-1})	A_{nrad} (s^{-1})	Ω_2 ($10^{-20}cm^2$)	Ω_4 ($10^{-20}cm^2$)	η (%)
C1 $[Eu(L)_3.2H_2O]$	0.3893	2568.71	201.45	2367.26	2.88	0.20	7.84
C2 $[Eu(L)_3.batho]$	1.2651	790.45	224.85	565.6	3.71	0.01	28.45
C3 $[Eu(L)_3.phen]$	1.5307	653.30	232.40	420.9	3.82	0.09	35.57
C4 $[Eu(L)_3.bipy]$	1.5706	636.70	233.59	403.11	3.88	0.05	36.69

τ (ms): luminescent lifetime in millisecond; A_{rad}: radiative rate constant; A_{nrad}: non-radiative rate constant; A_{total}: total radiative rate constant; η: internal quantum efficiency; Ω_2 and Ω_4: Judd–Ofelt parameters; L: 1-(4-methoxyphenyl)-5-(trifluoromethyl)-1*H*-pyrazole-4-carboxylic acid; batho: bathophenanthroline; phen: 1,10-phenanthroline; bipy: 2,2-bipyridyl.

respectively while A_{01} represents Einstein's coefficient of spontaneous emission for parity-allowed ($^5D_0 \rightarrow {}^7F_1$) transition which is independent of ligand field in the coordination sphere, therefore, it can be used as an internal reference and its value comes out to be about 50 s^{-1} in air.[35]

The Judd–Ofelt theory is put forward by Judd and Ofelt scientists, which is very helpful in investigation of asymmetric environment around metal ion and also determine the f-f electronic transitions by utilizing the Judd–Ofelt parameters Ω_λ ($\lambda = 2,\ 4$).[36] Ω_2 is primarily sensitive to chemical field created by the surrounding ligands, while Ω_4 mainly relies upon the metal–ligand distance which in turn related to rigidity of the system. Judd–Ofelt parameters (Ω_2 and Ω_4) are calculated by using the following equation:

$$\Omega_\lambda = 3\hbar c^3 A_{0J}/4e^2\omega^3\chi\langle {}^5D_0|U^{(\lambda)}|{}^7F_J\rangle^2 \qquad (9)$$

In the above equation, c denotes the velocity of light, $\hbar = h/2\pi$, h corresponds to Planck's constant, $\chi = n^2(n^2+2)^2/9$ represents the local field Lorentz correction term, e symbolizes the electronic charge (4.8×10^{-10} e.s.u.), and n signify the refractive index ($n = 1.5$). The term $\langle {}^5D_0|U^{(\lambda)}|{}^7F_J\rangle^2$ denotes the squares of reduced matrix element having values 0.0032 ($^5D_0 \rightarrow {}^7F_2$) and 0.0023 ($^5D_0 \rightarrow {}^7F_4$).[37] The calculated values of Ω_2 and Ω_4 for C1–C4 complexes are summarized in Table 4. Higher value of Ω_2 for C2–C4 complexes reflects the presence of more covalence character and asymmetric chemical environment around the europium(III) ion whereas greater value of Ω_4 reflects the high rigidity of C2–C4 complexes due to presence of auxiliary ligands in C2–C4 complexes.

Scanning electron microscopy analysis

The surface morphology of the particles is confirmed by SEM analysis which indicates that the particles possessed by the complexes are crystalline in nature. The particles morphology of all complexes is represented by SEM micrograph of C4 complex as manifested in Fig. 12, which demonstrates that the particles are crystalline in nature and some particles are seen in conglomerated stage.

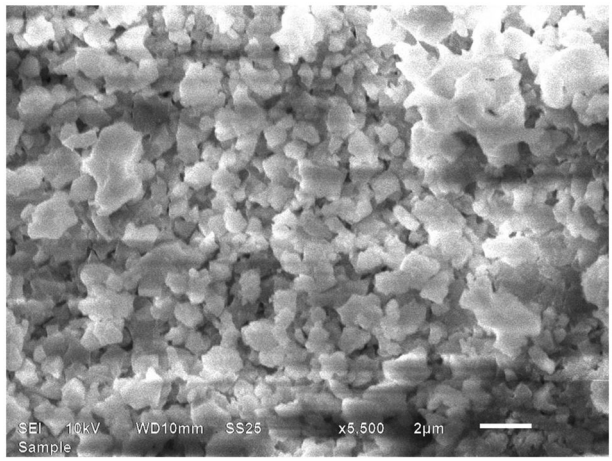

Figure 12. Scanning electron microscope image of C_4 complex of europium(III) ion with main ligand 1-(4-methoxyphenyl)-5-(trifluoromethyl)-1*H*-pyrazole-4-carboxylic acid and auxiliary ligand 2,2-bipyridyl. The image indicates the crystalline nature of particles which are possessed by complex C_4.

Analysis of biological activity

Antimicrobial properties

The antibacterial property of ligand (L) and its respective complexes are assessed against Gram-positive and Gram-negative bacterial pathogens such as *S. aureus* and *E. coli*, *P. aeruginosa*, respectively, by using ciprofloxacin as standard drug. The fungal pathogens like *A. niger* and *C. albicans* are used to determine the antifungal activity of complexes against fluconazole as standard drug. These antimicrobial activities are investigated in terms of MIC values as reported in Table 5 and represented by bar graph of C4 complex in Fig. 13. The recorded MIC values suggest that europium(III) complexes are acted as more potent than ligand (L) and reference drugs used. For *S. aureus*, C2 and C3 complexes (6.25 μg/mL) are more active than C1 and C4 complexes (12.5 μg/mL). Against *E. coli*, C2 complex (3.13 μg/mL) shows significantly greater activity and C3–C4 complexes (6.25 μg/mL) are moderate active whilst C1 complex (12.5 μg/mL) is inactive against this bacterial pathogen. In the case of *P. aeruginosa*, C2–C3 complexes (3.13 μg/mL) are more active than C1 and C4 complexes (6.25 μg/mL). It is clearly revealed that the order of antibacterial potential of the complexes is found to be C2 > C3 > C4 > C1.

Against *C. albicans*, C4 complex (3.13 μg/mL) is more active than other complexes

Table 5. Minimum inhibitory concentration values of main ligand 1-(4-methoxyphenyl)-5-(trifluoromethyl)-1*H*-pyrazole-4-carboxylic acid, complex C_1 of europium(III) ion with main ligand and complexes C_2–C_4 with main ligand and auxiliary ligands bathophenanthroline, 1,10-phenanthroline and 2,2-bipyridyl, respectively, determined against ciprofloxacin (bacteria) and fluconazole (fungi) standard drugs.

	Minimum inhibitory concentration (μg/mL)				
Complexes	MIC_{sa}	MIC_{ec}	MIC_{pa}	MIC_{ca}	MIC_{an}
L	12.5	12.5	12.25	25.0	12.5
C1 [$Eu(L)_3.2H_2O$]	12.5	12.5	6.25	6.25	12.5
C2 [$Eu(L)_3$.batho]	**6.25**	**3.13**	**3.13**	12.5	**3.13**
C3 [$Eu(L)_3$.phen]	**6.25**	6.25	**3.13**	12.5	6.25
C4 [$Eu(L)_3$.bipy]	12.5	6.25	6.25	**3.13**	6.25
SD 25.0[a]	12.5[a]	12.5[a]	25.0[b]	12.5[b]	

MIC: minimum inhibitory concentration; L: 1-(4-methoxyphenyl)-5-(trifluoromethyl)-1*H*-pyrazole-4-carboxylic acid; batho: bathophenanthroline; phen: 1,10-phenanthroline; bipy: 2,2-bipyridyl; sa: *Staphylococcus aureus*; ec: *Escherichia coli*; pa: Pseudomonas aeruginosa (bacterial pathogens) and ca: *Candida albicans*; an: *Aspergillus niger* (fungal pathogens); a: ciprofloxacin; b: fluconazole; SD: standard drugs; μg/mL: microgram per milliliter. The bold values represent the lowest minimum inhibitory concentrations and highest antimicrobial activities.

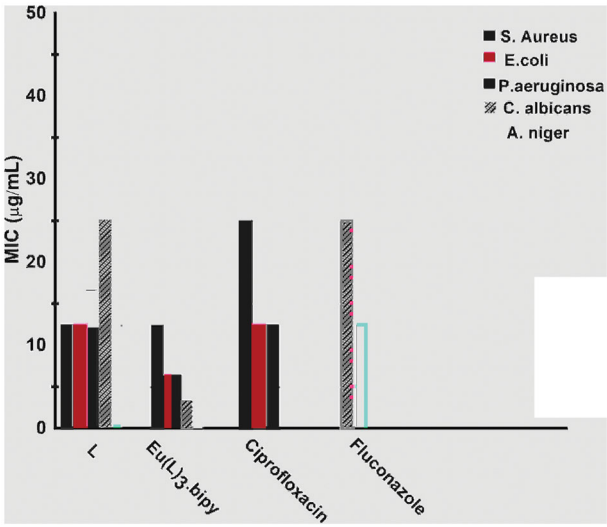

Figure 13. Antimicrobial activity of main ligand 1-(4-methoxyphenyl)-5-(trifluoromethyl)-1*H*-pyrazole-4-carboxylic acid and C_4 complex of europium(III) ion with main ligand and auxiliary ligand 2,2-bipyridyl investigated against the standard drugs, ciprofloxacin (bacteria), and fluconazole (fungi). The bar graph demonstrates that the ligand is less active agent than C_4 complex.

(6.25–12.5 μg/mL), while ligand L (25.0 μg/mL) is acted as inactive agent. Furthermore, the complex C2 (3.13 μg/mL) is excellent and C3–C4 complexes (6.25 μg/mL) are moderate antifungal agents against *A. niger* whereas C1 complex (12.5 μg/mL) are totally inactive against this fungal pathogen. It can be noted that the antimicrobial activity of C2 complex is comparatively greater than other complexes (C1, C3–C4), hence, this complex is considered as more powerful antimicrobial agent. It is noteworthy pointed that highly conjugated system of auxiliary ligand batho with nitrogen donor atoms increase the delocalization of π-electrons over the whole ligand, hence, it increases the lipid attracting tendency of Eu^{3+} ion. Thus, Eu^{3+} ion can be penetrated into the cell wall of microorganisms to a deep area, which consequently inhibits the growth of microbes and enhance the antimicrobial potential of complexes as compared to ligand (L) and reference drugs used.[38,39]

Antioxidant activity

Antioxidant activity of complexes and ligand (L) are determined by DPPH method. DPPH gets diamagnetic character by accepting the hydrogen radical from antioxidant complexes which results into absorbance of the complexes gets decrease and scavenging activity gets increased. A straight line graph is obtained between percentage scavenging activity (% SCA) and concentrations of samples, which is displayed in Fig. 14. Higher percentage scavenging activity (% SCA) of complexes increases the capability of complexes toward antioxidant activity. IC_{50} and percentage scavenging activity (% SCA) of the complexes are indexed in Table 6. It is clear from Table 6 that the free ligand L (IC_{50} = 61.92 μg/mL) is less active than standard ascorbic acid (IC_{50} = 46.71 μg/mL) and complexes C1–C4 (IC_{50} = 58.75–49.70 μg/mL). In the complexes, ligand donates its electron density to Eu^{3+} ion, hence, hydrogen atom gets easily ionized, which quench the DPPH activity and increase the antioxidant activity of complexes.[40] The antioxidant activity of C2–C4 complexes is enhanced through synergistic effect of auxiliary ligands.[41] The above fact suggests that the complexes C2–C4 are acted as an excellent antioxidant agent as compared to C1 complex and ligand (L).

Energy transfer mechanism

The emission spectral data is very helpful to interpret the energy transfer mechanism in the complexes and also ascertain the strength of photoemission signal of complexes. The mechanism involves the energy transfer from excited singlet level to triplet level of ligand (L) via

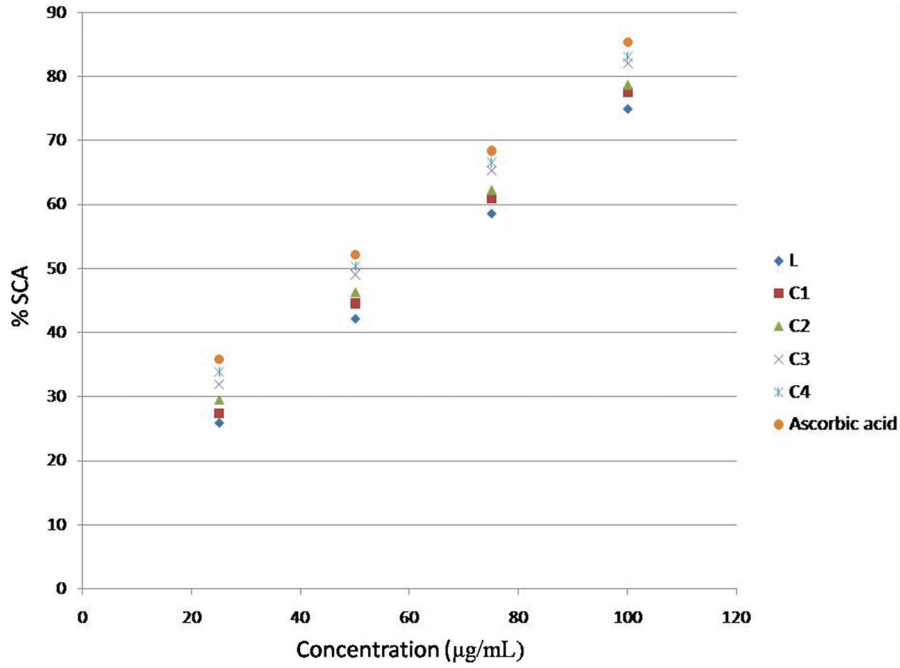

Figure 14. Variation of percentage scavenging activity with concentration for main ligand 1-(4-methoxyphenyl)-5-(trifluoromethyl)-1*H*-pyrazole-4-carboxylic acid, C_1 complex of europium(III) ion with main ligand and complexes C_2–C_4 with main ligand and auxiliary ligands such as bathophenanthroline, 1,10-phenanthroline and 2,2-bipyridyl, respectively, determined against ascorbic acid (standard). The graph clearly reveals that the complex C_4 is acted as an efficient antioxidant agent on the basis of percentage scavenging activity.

Table 6. The recorded percentage scavenging activity and 50% inhibitory concentration of free ligand 1-(4-methoxyphenyl)-5-(trifluoromethyl)-1*H*-pyrazole-4-carboxylic acid, C_1 complex of europium(III) ion with 1-(4-methoxyphenyl)-5-(trifluoromethyl)-1H-pyrazole-4-carboxylic acid as main ligand and C_2–C_4 complexes with main ligand and auxiliary ligands bathophenanthroline, 1,10-phenanthroline and 2,2-bipyridyl, respectively, against ascorbic acid (standard) at different concentrations.

	Concentration (μg/mL)				
Complexes	25	50	75	100	IC_{50}
L	25.86	42.12	58.58	74.96	61.92
C1 [$Eu(L)_3.2H_2O$]	27.35	44.47	60.88	77.43	58.75
C2 [$Eu(L)_3$.batho]	29.48	46.22	62.16	78.59	56.22
C3 [$Eu(L)_3$.phen]	31.95	49.04	65.31	82.02	51.94
C4 [$Eu(L)_3$.bipy]	33.81	50.29	66.55	83.11	49.70
Ascorbic acid	35.87	52.16	68.35	85.27	46.71

% SCA: percentage scavenging activity; IC_{50}: 50% inhibitory concentration; L: 1-(4-methoxyphenyl)-5-(trifluoromethyl)-1*H*-pyrazole-4-carboxylic acid; batho: bathophenanthroline, phen: 1,10-phenanthroline; bipy: 2,2-bipyridyl; μg/mL: microgram per milliliter. The highest antioxidant activity of complexes is confirmed by highest value of percentage scavenging activity.

intersystem crossing, finally to excited emissive levels (^5D_J) of Eu^{3+} ion through excited triplet level of ligand. The excited emissive level ($^5D_0$) gets relax to ground levels (^7F_J), which emit luminescence in visible region. The excited singlet (31,546 cm^{-1}) and triplet (24,752 cm^{-1}) energy levels of ligand (L) are determined by referring to their shortest edge wavelength of UV–vis absorption spectrum of ligand (L) (Fig. 5) and lowest emission band of phosphorescence spectrum of $Gd(L)_3.2H_2O$ complex (G1) (Fig. 15), respectively. The phosphorescence emission spectrum of G1 complex is ligand centered emission because the lowest emissive level of Gd^{3+} ion is positioned at about 32,000 cm^{-1}, which does not allow the transfer of energy from excited triplet level of ligand to emissive level of Gd^{3+} ion.[18] Similarly, the singlet and triplet energy levels of auxiliary ligands like bipy (S_1: 29,900 cm^{-1}, T_1: 22,900 cm^{-1}), phen (S_1: 31,000 cm^{-1}, T_1: 22,100 cm^{-1}), and batho (S_1: 29,000 cm^{-1}, T_1: 21,000 cm^{-1}) are determined, which are properly matched with the values reported in literature.[42] The energy transfer rate depends upon two main processes. In the first case, the energy transfer from lowest excited triplet level of ligand to emissive level of metal ion takes place according to Dexter's electron exchange interaction theory.[43] This theory proposed that more efficient energy transfer takes place, if more suitable energy gap is present between triplet level of ligand and emissive level of metal ion. The transfer

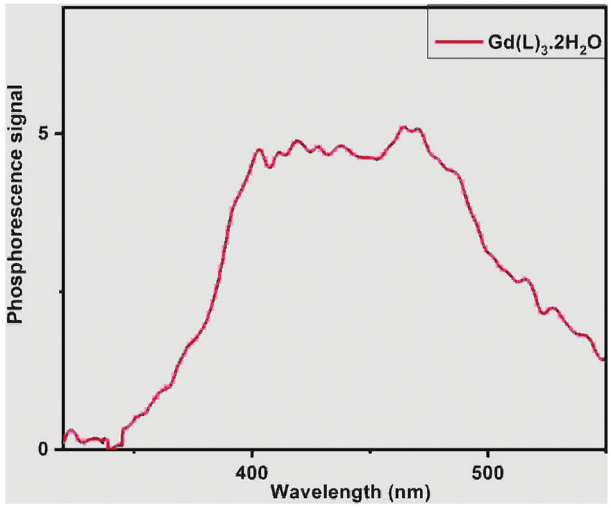

Figure 15. Phosphorescence spectrum of Gadolinium complex of ligand 1-(4-methoxyphenyl)-5-(trifluoromethyl)-1*H*-pyrazole-4-carboxylic acid in solid state. The energy of excited triplet level of ligand is determined from the lowest band wavelength (404 nm).

probability constant (P_s) is expressed as

$$P_S = \left(\frac{2\pi Z^2}{h}\right)\int F_S(E).\xi_s(E).dE \qquad (10)$$

Here, $F_S(E)$ represents the shape of emission band of energy donor triplet level of ligand, $\xi_s(E)$ shows the shape of absorption spectrum of energy acceptor metal ion and $2\pi Z^2/h$ term is constant. The second case deals with the thermal de-excitation or inverse energy transfer from metal ion to ligand, which can be represented as

$$K(T) = Ae^{\left(\frac{-\Delta E}{RT}\right)} \qquad (11)$$

Here, ΔE is energy difference between emissive level of metal ion and lowest excited triplet level of ligand and $K(T)$ is thermal de-excitation constant. Therefore, the value of transfer probability constant (P_S) decide the efficiency of energy transfer process from ligand to metal ion.

On the other hand, the scientist Reinhoudt proposed that the efficiency of intersystem crossing controlled by energy gap $\Delta E_1(S_1–T_1)$ between excited singlet (S_1) and triplet (T_1) level of ligand that should be at least 5000 cm^{-1}.[44] The value of ΔE_1 for ligand (L) is found to be 6794 cm^{-1} as demonstrated in Table 7, which permits the effective intersystem crossing in the complexes. The emissive levels of Eu^{3+} ion are positioned at 17,241, 18,657, and 21,368 cm^{-1} corresponding to $^5D_0 \rightarrow {}^7F_0$ (580 nm), $^5D_1 \rightarrow {}^7F_1$ (536 nm), and

Table 7. Energy (cm^{-1}) of excited levels of ligand 1-(4-methoxyphenyl)-5-(trifluoromethyl)-1*H*-pyrazole-4-carboxylic acid and auxiliary ligands bathophenanthroline, 1,10-phenanthroline and 2,2-bipyridyl.

Ligands	(S_1)	(T_1)	$\Delta E_1(S_1–T_1)$	$\Delta E(T_1–{}^5D_0)$	$\Delta E_2(T_1–{}^5D_1)$
L	31,546	24,752	6794	7511	6095
Bipy	29,900	22,900	7000	5659	4243
Phen	31,000	22,100	8900	4859	3443
Batho	29,000	21,000	8000	3759	2343

S_1 and T_1: lowest excited singlet and triplet energy levels of ligands, respectively; ΔE: energy difference; $^5D_0$ and $^5D_1$: excited energy levels of europium(III) ion; L: 1-(4-methoxyphenyl)-5-(trifluoromethyl)-1H-pyrazole-4-carboxylic acid; batho: bathophenanthroline, phen: 1,10-phenanthroline; bipy: 2,2-bipyridyl.

$^5D_2 \rightarrow {}^7F_0$ (468 nm) transitions, which are observed in emission spectra of complexes. The value of energy gap (T_1-Eu^{3+}) for different emissive levels of Eu^{3+} ion and ligand (L) are found to be 7511 ($^5D_0$), 6095 ($^5D_1$), and 3384 ($^5D_2$) cm^{-1}, which indicates that the ligand (L) transfer energy to $^5D_2$ level of Eu^{3+} ion as according to Latva empirical rule (T_1-Eu^{3+} = 2000–5000 cm^{-1}) and it sensitizes the Eu^{3+} ion.[45] The $^5D_2$ emissive level populates the $^5D_0$ level via non-radiative decay process, which in turn $^5D_0$ g relax to ground levels (^7F_J) radiatively and thus, emit luminescence in visible region. The excited triplet level of ligand (L) is located above the triplet level of auxiliary ligands, hence, its triplet level transfer energy to excited triplet level of auxiliary ligand, whereby the synergistic effect of auxiliary ligands intensify the emission signal of C2–C4 complexes than C1 complex. The energy values (ΔE_2) for bipy, phen, and batho are reckoned as 4243, 3443, and 2343 cm^{-1}, respectively, which clearly reveal that the ΔE_2 value for bipy auxiliary ligand is highest among all auxiliary ligands. Hence, this energy value (ΔE_2) for bipy negates the chance of inverse energy transfer from metal to ligand and exhibits the intense emission signal. On the contrary, the ΔE_2 value of batho is the lowest, which makes a possibility of inverse energy transfer and gets least intense emission signal among the auxiliary ligands. The proposed energy transfer mechanism of one of complex that is C4 is displayed in Fig. 16.

Conclusions

In this reported research work, four red color emitting europium(III) complexes (C1–C4) were synthesized by using main organic ligand, 1-(4-

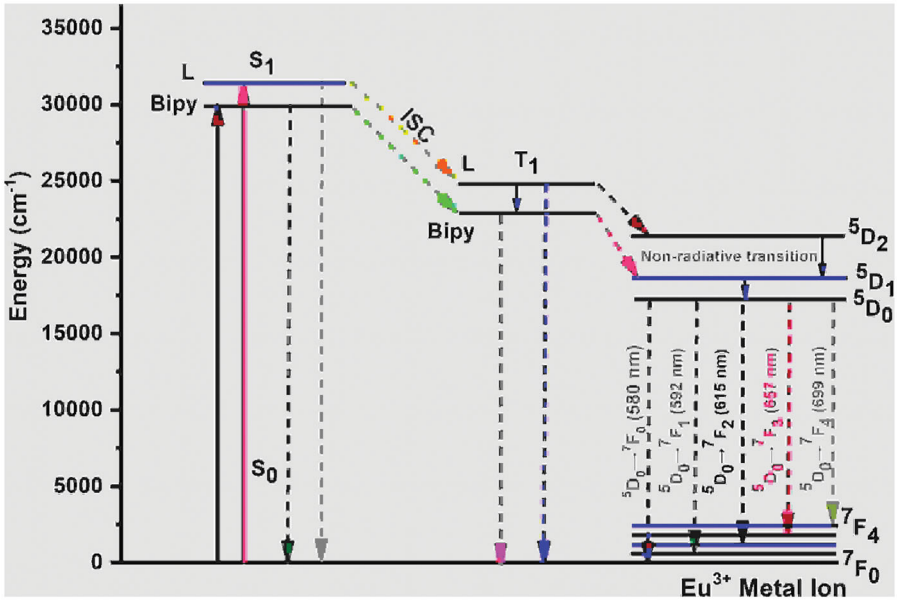

Figure 16. The schematic energy transfer mechanism in C_4 complex of europium(III) ion with main ligand 1-(4-methoxyphenyl)-5-(trifluoromethyl)-1*H*-pyrazole-4-carboxylic acid and auxiliary ligand 2,2-bipyridyl. It demonstrates the energy transfer from excited triplet level of main ligand and auxiliary ligand 2,2-bipyridyl to excited energy levels of europium(III) ion through different energy transfer pathways. The energy difference between triplet level of ligand L and $^5D_2$ of europium(III) ion is suitable for energy transfer process and auxiliary ligand also help in sensitization of europium(III) ion.

methoxyphenyl)-5-(trifluoromethyl)-1*H*-pyrazole-4-carboxylic acid (L) and auxiliary ligands through a more facile and less time consuming solution precipitation approach and characterized through various spectral techniques such as elemental and EDAX analyses, IR, NMR, DR, TG-DTG, and PL spectroscopy. The optical band-gap values of complexes (C2–C4) were found to be in the range of WBGs, which indicated their behavior like wide-band gap semiconductors and thus, proved better luminescent semiconductors than conventional semiconductors. TG-DTG study of complexes clearly revealed that the complexes possessed thermal stability up to 152 °C, which supported the role of them as emitting materials in OLEDs fabrication. SEM analysis affirmed the crystalline nature of particles, possessed by the complexes. The photoluminescence features of the complexes had been explored in detail, which suggested that the complexes have remarkable photoluminescence properties. The red emission of complexes was obtained at 614 (C1) and 615 (C2–C4) nm corresponding to $^5D_0 \rightarrow {}^7F_2$ transition of Eu^{3+} ion whereas CIE color coordinates were well situated in the red region reflected that the complexes play a great role in display devices. In addition, the energy transfer occurred more efficiently in C2–C4 complexes due to presence of auxiliary ligands which reduced the quenching produced by water molecules in C1 complex and also provided stability to the complexes, thereby, the luminescence efficiency of C2–C4 complexes was enhanced. The internal quantum efficiency (η) of europium(III) complexes increased from 7.84% to 36.69%, which was attributed to potential advantages of the complexes in lighting and display devices. Furthermore, the antimicrobial and antioxidant activity of complexes were also investigated via tube dilution and DPPH approach, respectively. The biological properties substantiated that the complexes were acted as best antimicrobial and antioxidant agents. The above characterization results proposed a promising role of the complexes in the fields of advanced luminescent devices, fabrication of white light emitting diodes, lasers, and solar technology.[46–49]

Ethics statement

- This is our original research work and it highlights new dimensions in the field of

luminescent materials and biological systems, by utilizing various advanced spectroscopic techniques. The work has not been published before; it is not under consideration for publication anywhere else; and publication has been approved by all coauthors and the responsible authorities at the institute(s) where the work has been carried out.

- Moreover, the authors are ready to follow all norms of the publications like copy right, etc.

Disclosure statement

No potential conflict of interest was reported by the author(s).

Funding

Authors are thankful to the University Grants Commission (UGC) for granting funds under special Assistance program [No. F.540/17/DRS-I/2016 SAP-I] to Department of Chemistry.

References

[1] Huijuan, R.; Dehui, S.; Zhenfeng, C.; Mei, Y.; Guangyan, H. Synthesis and Characterization of Terbium(III)-Pyromellitic Acid (H_4L)-1,10-Phenanthroline (Phen) Luminescent Complex. *Journal Rare Earths* **2010**, *28*, 47–50. DOI: 10.1016/S1002-0721(10)60384-5.

[2] Chen, W.; Li, M.; HuiBo, W.; ZhiWei, L.; ZuQiang, B.; ChunHui, H. Advances in Luminescent Lanthanide Complexes and Applications. *Science China-Technological Sciences* **2018**, *61*, 1265–1285. DOI: 10.1007/s11431-017-9212-7.

[3] Ilmi, R.; Khan, M. S.; Sun, W.; Zhou, L.; Wong, W. Y.; Raithby, P. R. A Single Component White Electroluminescent Device Fabricated from a Metallo-Organic Terbium Complex. *Journal of Materials Chemistry C* **2019**, *7*, 13966–13975. DOI: 10.1039/C9TC04653D.

[4] Bunzli, J. C. G. Rising Stars in Science and Technology: Luminescent Lanthanide Materials. *European Journal of Inorganic Chemistry* **2017**, *44*, 5058–5063. DOI: 10.1002/ejic.201701201.

[5] Piccinelli, F.; Bettinelli, M.; Melchior, A.; Grazioli, C.; Tolazzi, M. Structural, Optical and Sensing Properties of Novel Eu(III) Complexes with Furan- and Pyridine-*Based Ligands. *Dalton Transactions* **2015**, *44*, 182–192. DOI: 10.1039/C4DT02326A.

[6] Dossing, A. Luminescence from Lanthanide(3+) Ions in Solution. *European Journal of Inorganic Chemistry* **2015**, *8*, 1425–1434. DOI: 10.1002/ejic.200401043.

[7] Raj, D. B. A.; Biju, S.; Reddy, M. L. P. One-, Two-, and Three-Dimensional Arrays of Eu^{3+}-4,4,5,5,5-Pentafluoro-1-(Naphthalen-2-yl)Pentane-1,3-Dione Complexes: Synthesis, Crystal Structure and Photophysical Properties. *Inorganic Chemistry* **2008**, *47*, 8091–8100. DOI: 10.1021/ic8004757.

[8] Yue, B.; Chen, Y. N.; Chu, H. B.; Qu, Y. R.; Wang, A. L.; Zhao, Y. L. Synthesis, Crystal Structures and Fluorescence Properties of Dinuclear Tb(III) and Sm(III) Complexes with 2,4,6-Tri(2-Pyridyl)-1,3,5-Triazine and Halogenated Benzoic Acid. *Inorganica Chimica Acta* **2014**, *414*, 39–45. DOI: 10.1016/j.ica.2014.01.024.

[9] Bala, M.; Kumar, S.; Taxak, V. B.; Boora, P.; Khatkar, S. P. Synthesis, Photoluminescent Features and Intramolecular Energy Transfer Mechanism of Europium (III) Complexes with Fluorinate β-Diketone Ligand and Auxiliary Ligands. *Journal of Fluorine Chemistry* **2015**, *178*, 6–13. DOI: 10.1016/j.jfluchem.2015.06.011.

[10] Devi, R.; Priyanka Chahar, S.; Khatkar, S. P.; Taxak, V. B.; Boora, P. Judd Oflet Characterization and Energy Transfer Mechanism of Highly Luminescent Europium(III) Complexes with 1-(5-Chloro-2-Hydroxyphenyl)-1,3-Butanedione. *Inorganica Chimica Acta* **2018**, *471*, 364–371. DOI: 10.1016/j.ica.2017.11.006.

[11] Devi, R.; Chahar, S.; Khatkar, S. P.; Taxak, V. B.; Boora, P. Relative Study of Luminescent Properties with Judd-Ofelt Characterization in Trivalent Europium Complexes Comprising Ethyl-(4-Fluorobenzoyl) Acetate. *Journal of Fluorescence* **2017**, *27*, 1349–1358. DOI: 10.1007/s10895-017-2069-3.

[12] Dhankhar, P.; Devi, R.; Devi, S.; Chahar, S.; Dalal, M.; Taxak, V. B.; Khatkar, S. P.; Boora, P. Synthesis and Photoluminescent Performance of Novel Europium (III) Carboxylates with Heterocyclic Ancillary Ligands. *Rare Metals* **2019**. DOI: 10.1007/s12598-019-01261-y.

[13] Qiu, X. Synthesis and Evaluation of New Antimicrobial Agents and Novel Organic Fluorophores. PhD thesis, National University of Ireland, Maynooth, 2013, 24–26.

[14] Onawumi, O. O. E.; Odunola, O. A.; Suresh, E.; Paul, P. Synthesis, Structural Characterization and Microbial Activities of Mixed Ligand Copper(II) Complexes of 2,2′-Bipyridine and Acetylacetonate. *Inorganic Chemistry Communications* **2011**, *14*, 1626–1631. DOI: 10.1016/j.inoche.2011.06.025.

[15] Kardong, D.; Upadhyaya, S.; Saikia, L. R. Screening of Phytochemicals, Antioxidant and Antibacterial Activity of Crude Extract of Pteridium Aquilinum Kuhn. *Journal of Pharmacy Research* **2013**, *6*, 179–182. DOI: 10.1016/j.jopr.2012.11.037.

[16] Khullar, S.; Singh, S.; Das, P.; Mandal, S. K. Luminescent Lanthanide-*Based Probes for the Detection of Nitroaromatic Compounds in Water. *ACS Omega* **2019**, *4*, 5283–5292. DOI: 10.1021/acsomega.9b00223.

[17] Gao, B.; Qiao, Z.; Chen, T. Structure and Photoluminescence Property of Complexes of Aromatic Carboxylic Acid-Functionalized Polysulfone with Eu(III) and Tb(III). *Materials Chemistry and Physics* **2014**, *143*, 1119–1130. DOI: 10.1016/j.matchemphys.2013.11.012.

[18] Kharcheva, A. V.; Borisova, N. E.; Ivanov, A. V.; Reshetova, M. D.; Kaminskaya, T. P.; Popov, V. V.; Yuzhakov, V. I.; Patsaeva, S. V. Effect of Aliphatic Chain Length in the Ligand on Photophysical Properties and Thin Films Morphology of the Europium Complexes. *Russian Journal of Inorganic Chemistry* **2018**, *63*, 219–228. DOI: 10.1134/S0036023618020092.

[19] Shen, L.; Yang, Z.; Tang, R. Synthesis, Luminescence Properties of Eu(III) and Tb(III) Complexes with a Novel Aromatic Carboxylic Acid and Their Interactions with Bovine Serum Albumin. *Spectrochimica Acta Part A: Molecular and Biomolecular Spectroscopy* **2012**, *98*, 170–177. DOI: 10.1016/j.saa.2012.08.060.

[20] Sehrawat, P.; Khatkar, A.; Boora, P.; Kumar, M.; Malik, R. K.; Khatkar, S. P.; Taxak, V. B. Combustion derived color tunable Sm3+ activated BaLaAlO4 nanocrystals for various innovative solid stateilluminants. *Chemical Physics Letters* **2020**. DOI: 10.1016/j.cplett.2020.137937.

[21] Sehrawat, P.; Khatkar, A.; Devi, S.; Hooda, A.; Singh, S.; Malik, R. K.; Khatkar, S. P.; Taxak, V. B. An Effective Emission of Characteristic Cool White Light from Dy^{3+} Doped Perovskite Type $SrLa_2Al_2O_7$ Nanophosphors in Single-Phase Pc WLEDs. *Chemical Physics Letters* **2019**, *737*, 136842. DOI: 10.1016/j.cplett.2019.136842.

[22] Yan, L.; Popescu, F.; Rao, M. R.; Meng, H.; Perepichka, D. F. A Wide Band Gap Naphthalene Semiconductor for Thin-Film Transistors. *Advanced Electronic Materials* **2017**, *3*, 1600556–1600558. DOI: 10.1002/aelm.201600556.

[23] Dalal, J.; Dalal, M.; Devi, S.; Dhankhar, P.; Hooda, A.; Khatkar, A.; Taxak, V. B.; Khatkar, S. P. Structural and Judd-Ofelt Intensity Parameters of a Down-Converting $Ba_2GdV_3O_{11}$:Eu^{3+} Nanophosphors. *Materials Chemistry and Physics* **2020**, *243*, 122631. DOI: 10.1016/j.matchemphys.2020.122631.

[24] Dhankhar, P.; Bedi, M.; Khanagwal, J.; Taxak, V. B.; Khatkar, S. P.; Doon, P. B. Photoluminescent Report on Red Light Emitting Europium(III) Complexes with Heterocyclic Acid. *Spectroscopy Letters* **2020**, *53*, 256–269. DOI: 10.1080/00387010.2020.1736099.

[25] Liu, Y.; Liu, J.; Liu, Q.; He, W.; Kityk, I. V. Photophysical Spectral Features of Fluorescent Complexes on the Basis of the Novel Ligand *β*-Thujaplicin. *Journal of Luminescence* **2020**, *218*, 116852. DOI: 10.1016/j.jlumin.2019.116852.

[26] Gangan, T. V. U.; Sreenadh, S.; Reddy, M. L. P. Visible-Light Excitable Highly Luminescent Molecular Plastic Materials Derived from Eu^{3+}-Biphenyl Based *β*-Diketonate Ternary Complex and Poly(Methylmethacrylate). *Journal of Photochemistry and Photobiology A* **2016**, *328*, 171–181. DOI: 10.1016/j.jphotochem.2016.06.005.

[27] Wang, X.; Sun, K.; Wang, L.; Tian, X.; Zhang, Q.; Chen, B. Effect on the Fluorescence Branching Ratio of Different Synergistic Ligands in Neodymium Complex Doped PMMA. *Journal of Non-Crystalline Solids* **2012**, *358*, 1506–1510. DOI: 10.1016/j.jnoncrysol.2012.04.006.

[28] Guo, F.; Karl, A.; Xue, Q. F.; Tam, K. C.; Forberich, K.; Brabec, C. J. The Fabrication of Color-Tunable Organic Light-Emitting Diode Displays via Solution Processing. *Light: Science & Applications* **2017**, *6*, e17094. DOI: 10.1038/lsa.2017.94.

[29] Sehrawat, P.; Khatkar, A.; Boora, P.; Kumar, M.; Malik, R. K.; Khatkar, S. P.; Taxak, V. B. Emanating Cool White Light Emission from Novel Down-Converted $SrLaAlO_4$:Dy^{3+} Nanophosphors for Advanced Optoelectronic Applications. *Ceramics International* **2020**, *46*, 16274–16284. DOI: 10.1016/j.ceramint.2020.03.184.

[30] SeethaLekshmi, S.; Ramya, A. R.; Reddy, M. L. P.; Varughese, S. Lanthanide Complex-Derived White-Light Emitting Solids: A Survey on Design Strategies. *Journal of Photochemistry and Photobiology C* **2017**, *33*, 109–131. DOI: 10.1016/j.jphotochemrev.2017.11.001.

[31] Sehrawat, P.; Khatkar, A.; Boora, P.; Hooda, A.; Kumar, M.; Malik, R. K.; Khatkar, S. P.; Taxak, V. B. A Novel Strategy for High Color Purity Virescent Er^{3+}-Doped $SrLaAlO_4$ Nanocrystals for Solid-State Lighting Applications. *Journal of Materials Science: Materials in Electronics* **2020**, *31*, 6072–6083. DOI: 10.1007/s10854-020-03160-w.

[32] Francis, B.; Heering, C.; Freire, R. O.; Reddy, M. L. P.; Janiak, C. Achieving Visible-Light Excitation in Carbazole-Based Eu3+–b-Diketonate Complexes via Molecular Engineering. *RSC Advances* **2015**, *5*, 90720–90730. DOI: 10.1039/C5RA18819A.

[33] Werts, M. H. V.; Jukes, R. T. F.; Verhoeven, J. W. The Emission Spectrum and the Radiative Lifetime of Eu^{3+} in Luminescent Lanthanide Complexes. *Physical Chemistry Chemical Physics* **2002**, *4*, 1542–1548. DOI: 10.1039/b107770h.

[34] Yan, B. M.; Guo, M. Photofunctional Eu^{3+}/Tb^{3+} Organic-Inorganic Polymeric Hybrid Microsphere with Covalently Bonded Resin Hosts. *Journal of Photochemistry and Photobiology A* **2013**, *257*, 34–43. DOI: 10.1016/j.photochem.2013.02.013.

[35] Yan, B.; Lu, H. F. Lanthanide-Centered Inorganic/Organic Hybrids from Functionalized 2-Pyrrolidinone-5-Carboxylic Acid Bridge: Covalently Bonded Assembly and Luminescence. *The Journal of Organometallic Chemistry* **2009**, *694*, 2597–2603. DOI: 10.1016/j.jorganchem.2009.03.048.

[36] de Sá, G. F.; Malta, O. L.; de Mello Donegá, C.; Simas, A. M.; Longo, R. L.; Santa-Cruz, P. A.; da Silva, E. F. Spectroscopic Properties and Design of Highly Luminescent Lanthanide Coordination Complexes. *Coordination Chemistry Reviews* **2000**, *196*, 165–195. DOI: 10.1016/S0010-8545(99)00054-5.

[37] Hasegawa, Y.; Wada, Y.; Yanagida, S. Strategies for the Design of Luminescent Lanthanide(III) Complexes and Their Photonic Applications. *Journal of Photochemistry and Photobiology C* **2004**, *5*, 183–202. DOI: 10.1016/j.jphotochemrev.2004.10.003.

[38] Ferreira, R. A.; S; Nobre, S. S.; Granadeiro, C. M.; Nogueira, H. I. S.; Carlos, L. D.; Malta, O. L. A Theoretical Interpretation of the Abnormal $^5D_0 \rightarrow {}^7F_4$ Intensity Based on the Eu^{3+} Local Coordination in the $Na_9[EuW_{10}O_{36}]\cdot 14H_2O$ Polyoxometalate. *Journal of Luminescence* **2006**, *121*, 561–567. DOI: 10.1016/j.jlumin.2005.12.044.

[39] Ajlouni, A. M.; Taha, Z. A.; Momani, W. A.; Hijazi, A. K.; Ebqa'ai, M. Synthesis, Characterization, Biological Activities, and Luminescent Properties of Lanthanide Complexes with N, N′-Bis (2-Hydroxy-1-Naphthylidene)-1, 6-Hexadiimine. *Inorganica Chimica Acta* **2012**, *388*, 120–126. DOI: 10.1016/j.ica.2012.03.029.

[40] Hossain, S.; Zakaria, C. M.; Kudrat-E-Zahan, M. Metal Complexes as Potential Antimicrobial Agent: A Review. *American Journal of Heterocyclic Chemistry* **2018**, *4*, 1–21. DOI: 10.11648/j.ajhc.20180401.11.

[41] Ajlouni, A. M.; Salem, Q. A.; Taha, Z. A.; Hijazi, A. K.; Momani, W. A. Synthesis, Characterization, Biological Activities and Luminescent Properties of Lanthanide Complexes with [2-Thiophenecarboxylic Acid, 2-(2-Pyridinylmethylene)Hydrazide] Schiff Bases Ligand. *Journal of Rare Earths* **2016**, *34*, 986–993. DOI: 10.1016/S1002-0721(16)60125-4.

[42] Ravichandran, J.; Gurumoorthy, P.; Musthafa, M. A. I.; Rahiman, A. K. Antioxidant, DNA Binding and Nuclease Activities of Heteroleptic Copper(II) Complexes Derived from 2-((2-(Piperazin-1-yl)Ethylimino)methyl)-4-Substituted Phenols and Diimines. *Spectrochimica Acta. Part A, Molecular and Biomolecular Spectroscopy* **2014**, *133*, 785–793. DOI: 10.1016/j.saa.2014.06.045.

[43] Wan, Y.; Lyu, H.; Du, H.; Wang, D.; Yin, G. Synthesis and Photophysical Properties of Europium Pentafluorinated β-Diketonate Complexes. *Research on Chemical Intermediates* **2019**, *45*, 1669–1687. DOI: 10.1007/s11164-018-3691-7.

[44] Bala, M.; Kumar, S.; Taxak, V. B.; Boora, P.; Khatkar, S. P. Terbium(III) Complexes Sensitized with β-Diketone and Ancillary Ligands: Synthesis, Elucidation of Photoluminescence Properties and Mechanism. *Journal of Materials Science: Materials in Electronics* **2016**, *27*, 9306–9313. DOI: 10.1007/s10854-016-4970-y.

[45] Steemers, F. J.; Verboom, W.; Reinhoudt, D. N.; van der Tol, E. B.; Verhoeven, J. W. New Sensitizer-Modified Calix[4]Arene Enabling near-UV Excitation of Complexed Luminescent Lanthanide Ions. *The Journal of the American Chemical Society* **1995**, *117*, 9408–9414. DOI: 10.1021/ja00142a004.

[46] Latva, M.; Takalo, H.; Mukkala, V. M.; Matachescu, C.; Rodríguez-Ubis, J. C.; Kankare, J. Correlation between the Lowest Triplet State Energy Level of the Ligand and Lanthanide(III) Luminescence Quantum Yield. *Journal of Luminescence* **1997**, *75*, 149–169. DOI: 10.1016/S0022-2313(97)00113-0.

[47] Sehrawat, P.; Khatkar, A.; Boora, P.; Khanagwal, J.; Kumar, M.; Malik, R. K.; Khatkar, S. P.; Taxak, V. B. Tailoring the Tunable Luminescence from Novel Sm^{3+} Doped SLAO Nanomaterials for NUV-Excited WLEDs. *Chemical Physics Letters* **2020**, *755*, 137758. DOI: 10.1016/j.cplett.2020.137758.

[48] Sehrawat, P.; Khatkar, A.; Boora, P.; Kumar, M.; Singh, S.; Malik, R. K.; Khatkar, S. P.; Taxak, V. B. Fabrication of Single-Phase $BaLaAlO_4:Dy^{3+}$ Nanophosphors by Combustion Synthesis. *Materials and Manufacturing Processes* **2020**, *35*, 1259–1267. DOI: 10.1080/10426914.2020.1762206.

[49] Sehrawat, P.; Khatkar, A.; Devi, S.; Kumar, R.; Malik, R. K.; Khatkar, S. P.; Taxak, V. B. Crystal Structure and Photophysical Features of Greenish Perovskite Type $SrLa_2Al_2O_7:Er^{3+}$ Nanocrystals for down Conversion White LEDs. *Materials Research Express* **2020**, *6*, 126213. DOI: 10.1088/2053-1591/ab6653.

[50] Sehrawat, P.; Khatkar, A.; Hooda, A.; Kumar, M.; Kumar, R.; Malik, R. K.; Khatkar, S. P.; Taxak, V. B. An Energy-Efficient Novel Emerald Er^{3+} Doped $SrGdAlO_4$ Nanophosphor for PC WLEDs Excitable by NUV Light. *Ceramics International* **2019**, *45*, 24104–24114. DOI: 10.1016/j.ceramint.2019.08.118.